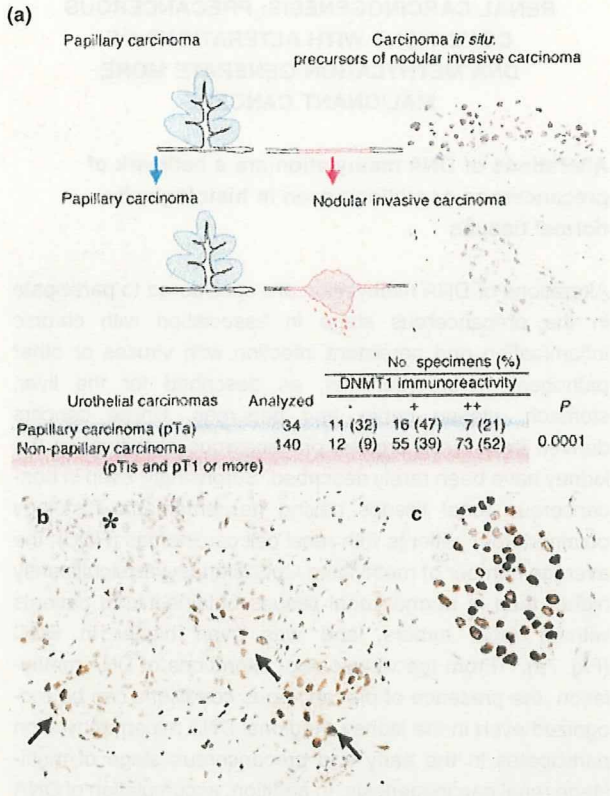

Figure 6 Immunohistochemistry of DNA methyltransferase 1 (DNMT1) in urothelial carcinomas. (**a**) The incidence and intensity of nuclear DNMT1 immunoreactivity were significantly higher in nodular invasive carcinomas with aggressive clinical courses and carcinomas *in situ*, which are considered to be precursor lesions of nodular invasive carcinoma, than in papillary carcinomas, which usually remain non-invasive.[76] +, >30% of the cells had the same nuclear staining intensity as the positive internal control lymphocytes; ++, >30% of the cells had stronger intensity. (**b**) In invasive carcinomas, cancer cells occasionally have particularly strong nuclear DNMT1 immunoreactivity at the invading front (arrows) or (**c**) in involved lymphatic vessels.[76] (*) Center of the cancer nest.

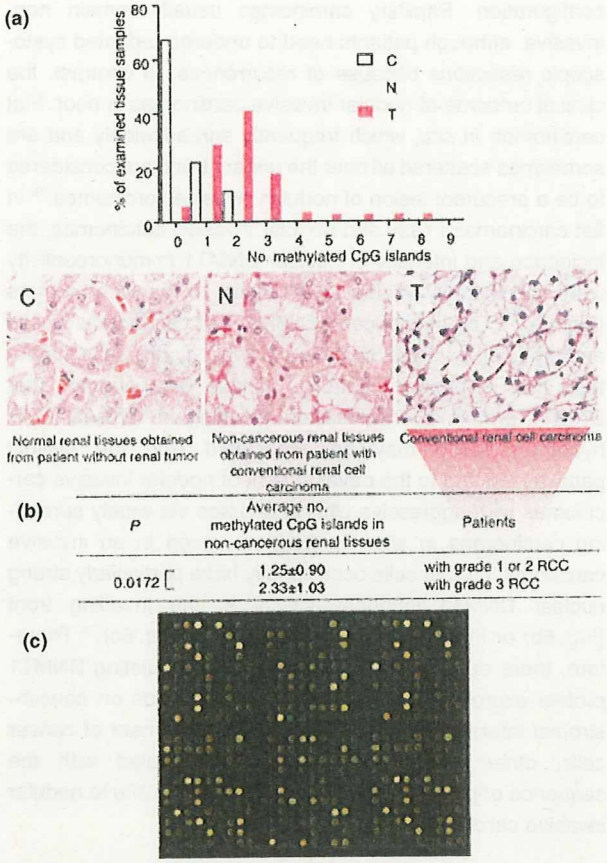

Figure 7 Precancerous conditions with alterations of DNA methylation generate more malignant renal cell carcinomas (RCC). (**a**) Even though non-cancerous renal tissues obtained from patients with renal cell carcinomas lacked remarkable histology (N), the average number of methylated CpG islands was significantly higher in N than in normal renal tissues obtained from patients without renal tumors (C).[80] The average number of methylated CpG islands was even higher in renal cell carcinomas (T).[80] (**b**) The average number of methylated CpG islands in N was significantly correlated with a higher histological grade of corresponding renal cell carcinomas developing in individual patients,[80] suggesting that regional DNA hypermethylation in precancerous conditions generates more malignant renal cell carcinomas. (**c**) Example of hybridization in the bacterial artificial chromosome array-based methylated CpG island amplification (BAMCA) method using MCG Whole Genome Array-4500 constructed by Dr Johji Inazawa, Tokyo Medical and Dental University, Tokyo, Japan and Dr Misao Ohki and Dr Fumie Hosoda, National Cancer Center Research Institute, Tokyo, Japan. This technique allows high resolution and genome-wide analysis of DNA methylation status, and suggests that the future development of more malignant RCC is determined by the genome-wide DNA methylation profile at the precancerous stage.

lia and urothelial carcinomas, concurrent DNA hypermethylation of three or more examined C-type CpG islands was significantly correlated with overexpression of DNMT1 protein.[77] Further examination is required to clarify the molecular mechanisms of recruitment of DNMT1 in a sequence-specific manner during carcinogenesis.

Alterations of DNA methylation participate particularly in the development of nodular invasive carcinomas via widely spreading carcinomas *in situ*

Although the incidence and intensity of nuclear DNMT1 immunoreactivity are correlated significantly with the histological grade of urothelial carcinomas, they appear not to be simply correlated with the depth of invasion.[76] Therefore, the morphological structures of urothelial carcinomas were examined (Fig. 6a). Urinary bladder cancers are classified as papillary or nodular according to their macroscopic

configuration. Papillary carcinomas usually remain non-invasive, although patients need to undergo repeated cystoscopic resections because of recurrences. In contrast, the clinical outcome of nodular invasive carcinomas is poor. Flat carcinomas *in situ*, which frequently spread widely and are sometimes scattered all over the urinary tract, are considered to be a precursor lesion of nodular invasive carcinomas.[78] In flat carcinomas *in situ* and nodular invasive carcinomas, the incidence and intensity of nuclear DNMT1 immunoreactivity were significantly higher than those in papillary tumors (Fig. 6a).[76] The incidence of CIMP in flat carcinomas *in situ* and nodular invasive carcinomas was significantly higher than that in papillary tumors.[77] These data suggest that DNMT1 protein overexpression resulting in regional DNA hypermethylation may be associated with the distinct pathway leading to the development of nodular invasive carcinomas with aggressive clinical courses via widely spreading carcinomas *in situ*. Furthermore, even in an invasive carcinoma, cancer cells occasionally have particularly strong nuclear DNMT1 immunoreactivity at the invading front (Fig. 6b) or in involved lymphatic vessels (Fig. 6c).[76] Therefore, there appears to be a mechanism regulating DNMT1 protein expression, possibly one that depends on cancer–stromal interactions and/or the microenvironment of cancer cells, other than the mechanism associated with the sequence of progression of flat carcinomas *in situ* to nodular invasive carcinomas.

DNA hypomethylation in pericentromeric satellite regions significantly correlates with chromosomal instability

DNA hypomethylation on satellites 2 and 3 was frequently detected in urothelial carcinomas of the urinary bladder, the ureter or the renal pelvis.[79] In almost all the carcinoma samples in which DNA hypomethylation was detected, hypomethylation occurred on both satellites 2 and 3. The incidence of DNA hypomethylation in pericentromeric satellite regions was significantly correlated with histological grade of urothelial carcinomas and was higher in nodular invasive carcinomas than in papillary tumors.[79] Satellites 2 and 3 are abundant in pericentromeric heterochromatin regions on chromosome 9. The incidence of LOH on chromosome 9 was significantly correlated with the histological grade of urothelial carcinomas and was higher in nodular invasive carcinomas than in papillary tumors.[79] DNA hypomethylation in pericentromeric satellite regions was significantly correlated with the presence of LOH on chromosome 9 in urothelial carcinomas,[79] suggesting that DNA hypomethylation inducing chromosomal instability may participate in urothelial carcinogenesis.

RENAL CARCINOGENESIS: PRECANCEROUS CONDITIONS WITH ALTERATIONS OF DNA METHYLATION GENERATE MORE MALIGNANT CANCERS

Alterations of DNA methylation are a hallmark of precancerous conditions even in histologically normal tissues

Alterations of DNA methylation are considered to participate in the precancerous stage in association with chronic inflammation and persistent infection with viruses or other pathogenic microorganisms, as described for the liver, stomach, uterine cervix and pancreas. Unlike cancers derived from these organs, precancerous conditions in the kidney have been rarely described. Surprisingly, even in non-cancerous renal tissues having no remarkable histology obtained from patients with renal cell carcinomas (RCC), the average number of methylated CpG islands was significantly higher than in normal renal tissues obtained from patients without renal tumors, and was even higher in RCC (Fig. 7a).[80] From the viewpoint of alterations of DNA methylation, the presence of precancerous conditions can be recognized even in the kidney. Regional DNA hypermethylation participates in the early and precancerous stage of multistage renal carcinogenesis. In addition, accumulation of DNA methylation at CpG islands in conventional RCC is significantly correlated with higher histological grade, an infiltrating growth pattern, and vascular involvement,[80] suggesting that regional DNA hypermethylation is continuously involved in malignant progression. The recurrence-free survival rate of patients with conventional RCC having accumulated DNA methylation of CpG islands was significantly lower than that of patients with conventional RCC lacking this feature.[80]

Genome-wide analysis indicates the significance of alterations of DNA methylation in precancerous conditions

The average number of methylated CpG islands in non-cancerous renal tissues lacking remarkable histology obtained from patients with conventional RCC was significantly correlated with a higher histological grade of corresponding RCC developing in individual patients (Fig. 7b).[80] These are striking data suggesting the possibility that regional DNA hypermethylation in precancerous conditions generates more malignant RCC. Examination of the DNA methylation status of only a restricted number of C-type CpG islands, however, cannot clarify whether DNA methylation status in restricted regions is simply altered in the precancerous stage or whether the genome-wide DNA methylation profile in the precancerous stage determines the clinico-

pathological characteristics of developing cancers. Recently, several techniques such as restriction landmark genomic scanning, methylation-sensitive representational difference analysis, methylated CpG island amplification and array-based technology have been developed for genome-wide analysis of DNA methylation status.[81–85] For DNA methylation profiling during multistage renal carcinogenesis, we used bacterial artificial chromosome (BAC) array-based methylated CpG island amplification (BAMCA, Fig. 7c).[86] Many researchers use arrays in which the promoter regions are enriched, as probes for cloning genes that are differentially methylated between cancer cells and normal cells. But the promoter regions of specific genes are not the only target of alterations of DNA methylation in human cancers. DNA methylation status in genomic regions not affecting the expression of specific genes may be altered before the alterations of the promoter regions themselves at the precancerous stage. Genomic regions in which DNA methylation status affects chromosomal instability are not contained in promoter-arrays. To obtain a high-resolution genome-wide overview of DNA methylation status, the BAMCA method was used, focusing not only on the promoter regions. In non-cancerous renal tissues lacking remarkable histology, obtained from patients with conventional RCC, the number of BAC clones having DNA hypermethylation or hypomethylation exceeding individual variation was significantly correlated with the recurrence-free survival rate of patients after nephrectomy for established RCC (Arai E. *et al.*, unpubl. data, 2008). These data suggest that the future development of more malignant RCC is determined by the genome-wide DNA methylation profile at the precancerous stage.

PERSPECTIVES

In earlier days it was thought, mistakenly, that alterations of DNA methylation occurred only as a result of cancerization. But because alterations of DNA methylation occur even in the precancerous stage before the establishment of cancer and determine the clinicopathological characteristics of the developing malignancies, it is clear that they are not a secondary result of cancerization. Precancerous conditions involving alterations of DNA methylation may generate more malignant cancers. Alterations of DNA methylation are frequently observed in precancerous conditions associated with chronic inflammation and/or persistent infection with viruses or other pathogenic microorganisms, such as HBV or HCV, EBV, HPV and *Helicobacter pylori*, or with cigarette smoking. When estimating carcinogenetic risk using DNA methylation profiles as indicators, elimination of such etiological factors may be efficient for cancer prevention. Moreover, DNA methylation is reversible, thus differing from genetic events during multistage carcinogenesis, and regional DNA hypermethylation can be corrected by passive demethylation with demethylating agents. Therefore, carcinogenetic risk estimation may pave the way to chemoprevention of precancerous conditions characterized by alterations of DNA methylation.

Early diagnosis of cancers using DNA methylation profiles as indicators is also a promising avenue. For this purpose, less invasive methodologies for detecting subtle alterations of DNA methylation should be developed for serum, urine, sputum and other body fluid samples. Because even subtle alterations of DNA methylation in the early stage are stably preserved on DNA double strands by covalent bonds, alterations of DNA methylation on appropriate genes and/or DNA fragments may be better indicators for early diagnosis than levels of mRNA and protein expression of specific genes that can be easily affected by the microenvironment of precursor cells or cancer cells.

Alterations of DNA methylation seem to continuously participate in the malignant progression of cancers by inducing chromosomal instability and silencing tumor-suppressor genes. Overexpression of DNMT1 is not a secondary result of increased cell proliferative activity but is significantly correlated with CIMP. DNA methylation profiles of not only normal tissues but also cancers tend to be organ-specific, and hot spots of DNA hypermethylation may reflect the diversity of carcinogenetic factors. The molecular mechanisms responsible for determination of the target genes of CIMP should be further clarified. Because alterations of DNA methylation and overexpression of DNMT1 are significantly associated with poorer tumor differentiation, tumor aggressiveness, and poorer patient outcome, estimation of DNA methylation status or immunohistochemistry of DNMT1 in biopsy specimens and/or surgically resected materials may also become a useful tool for prognostication. In contrast, splicing alteration of DNMT3B may result in chromosomal instability through DNA hypomethylation in pericentromeric satellite regions.

Recently developed technologies for accessing genome-wide DNA methylation status will be useful for identifying the DNA methylation profile, which is the optimum indicator of prognosis. Reactivation of tumor-suppressor genes by demethylating agents can provide a strategy of cancer therapy.[87] But overall DNA hypomethylation and regional DNA hypermethylation are commonly observed during multistage carcinogenesis, and they do not seem mutually exclusive in an individual patient. Therefore, before using DNA demethylation agents for prevention or therapy of cancers, it will be necessary to carefully identify patients who might benefit from this type of demethylation strategy. Accessing genome-wide DNA methylation status again seems indispensable for identification of patients whose cancers have a demethylating agent-sensitive DNA methylation profile.

ACKNOWLEDGMENTS

This work was supported by a Grant-in-Aid for the Third Term Comprehensive 10 Year Strategy for Cancer Control and a Grant-in-Aid for Cancer Research from the Ministry of Health, Labor and Welfare of Japan, and the Program for Promotion of Fundamental Studies in Health Sciences of the National Institute of Biomedical Innovation (NiBio).

REFERENCES

1 Holliday R. The inheritance of epigenetic defects. *Science* 1987; **238**: 163–70.
2 Esteller M. Epigenetics in cancer. *N Engl J Med* 2008; **358**: 1148–59.
3 Miranda TB, Jones PA. DNA methylation: The nuts and bolts of repression. *J Cell Physiol* 2007; **213**: 384–90.
4 Reik W. Stability and flexibility of epigenetic gene regulation in mammalian development. *Nature* 2007; **447**: 425–32.
5 Bestor T, Laudano A, Mattaliano R, Ingram V. Cloning and sequencing of a cDNA encoding DNA methyltransferase of mouse cells. The carboxyl-terminal domain of the mammalian enzymes is related to bacterial restriction methyltransferases. *J Mol Biol* 1988; **203**: 971–83.
6 Yoder JA, Bestor TH. A candidate mammalian DNA methyltransferase related to pmt1p of fission yeast. *Hum Mol Genet* 1998; **7**: 279–84.
7 Okano M, Xie S, Li E. Cloning and characterization of a family of novel mammalian DNA (cytosine-5) methyltransferases. *Nat Genet* 1998; **19**: 219–20.
8 Li E, Bestor TH, Jaenisch R. Targeted mutation of the DNA methyltransferase gene results in embryonic lethality. *Cell* 1992; **69**: 915–26.
9 Hermann A, Gowher H, Jeltsch A. Biochemistry and biology of mammalian DNA methyltransferases. *Cell Mol Life Sci* 2004; **61**: 2571–87.
10 Bestor TH. The DNA methyltransferases of mammals. *Hum Mol Genet* 2000; **9**: 2395–402.
11 Rountree MR, Bachman KE, Baylin SB. DNMT1 binds HDAC2 and a new co-repressor, DMAP1, to form a complex at replication foci. *Nat Genet* 2000; **25**: 269–77.
12 Robertson KD, Ait-Si-Ali S, Yokochi T, Wade PA, Jones PL, Wolffe AP. DNMT1 forms a complex with Rb, E2F1 and HDAC1 and represses transcription from E2F-responsive promoters. *Nat Genet* 2000; **25**: 338–42.
13 Clouaire T, Stancheva I. Methyl-CpG binding proteins: Specialized transcriptional repressors or structural components of chromatin? *Cell Mol Life Sci* 2008; **65**: 1509–22.
14 Bestor TH. Activation of mammalian DNA methyltransferase by cleavage of a Zn binding regulatory domain. *EMBO J* 1992; **11**: 2611–17.
15 Chuang LS, Ian HI, Koh TW, Ng HH, Xu G, Li BF. Human DNA-(cytosine-5) methyltransferase-PCNA complex as a target for p21WAF1. *Science* 1997; **277**: 1996–2000.
16 Okano M, Bell DW, Haber DA, Li E. DNA methyltransferases Dnmt3a and Dnmt3b are essential for de novo methylation and mammalian development. *Cell* 1999; **99**: 247–57.
17 Hansen RS, Wijmenga C, Luo P *et al.* The DNMT3B DNA methyltransferase gene is mutated in the ICF immunodeficiency syndrome. *Proc Natl Acad Sci USA* 1999; **96**: 14412–17.
18 Vertino PM, Yen RW, Gao J, Baylin SB. De novo methylation of CpG island sequences in human fibroblasts overexpressing DNA (cytosine-5-)-methyltransferase. *Mol Cell Biol* 1996; **16**: 4555–65.
19 Rhee I, Bachman KE, Park BH *et al.* DNMT1 and DNMT3b cooperate to silence genes in human cancer cells. *Nature* 2002; **416**: 552–6.
20 Hata K, Okano M, Lei H, Li E. Dnmt3L cooperates with the Dnmt3 family of de novo DNA methyltransferases to establish maternal imprints in mice. *Development* 2002; **129**: 1983–93.
21 Jones PL, Veenstra GJ, Wade PA *et al.* Methylated DNA and MeCP2 recruit histone deacetylase to repress transcription. *Nat Genet* 1998; **19**: 187–91.
22 Nan X, Ng HH, Johnson CA *et al.* Transcriptional repression by the methyl-CpG-binding protein MeCP2 involves a histone deacetylase complex. *Nature* 1998; **393**: 386–9.
23 Sarraf SA, Stancheva I. Methyl-CpG binding protein MBD1 couples histone H3 methylation at lysine 9 by SETDB1 to DNA replication and chromatin assembly. *Mol Cell* 2004; **15**: 595–605.
24 Ng HH, Zhang Y, Hendrich B *et al.* MBD2 is a transcriptional repressor belonging to the MeCP1 histone deacetylase complex. *Nat Genet* 1999; **23**: 58–61.
25 Zhang Y, Ng HH, Erdjument-Bromage H, Tempst P, Bird A, Reinberg D. Analysis of the NuRD subunits reveals a histone deacetylase core complex and a connection with DNA methylation. *Genes Dev* 1999; **13**: 1924–35.
26 Hendrich B, Hardeland U, Ng HH, Jiricny J, Bird A. The thymine glycosylase MBD4 can bind to the product of deamination at methylated CpG sites. *Nature* 1999; **401**: 301–4.
27 Jones PA, Baylin SB. The fundamental role of epigenetic events in cancer. *Nat Rev Genet* 2002; **3**: 415–28.
28 Laird PW. The power and the promise of DNA methylation markers. *Nat Rev Cancer* 2003; **3**: 253–66.
29 Ushijima T. Detection and interpretation of altered methylation patterns in cancer cells. *Nat Rev Cancer* 2005; **5**: 223–31.
30 Kanai Y, Hirohashi S. Alterations of DNA methylation associated with abnormalities of DNA methyltransferases in human cancers during transition from a precancerous to a malignant state. *Carcinogenesis* 2007; **28**: 2434–42.
31 Baylin SB, Ohm JE. Epigenetic gene silencing in cancer: A mechanism for early oncogenic pathway addiction? *Nat Rev Cancer* **2006**; **6**: 107–16.
32 Laird PW, Jackson-Grusby L, Fazeli A *et al.* Suppression of intestinal neoplasia by DNA hypomethylation. *Cell* 1995; **81**: 197–205.
33 Eden A, Gaudet F, Waghmare A, Jaenisch R. Chromosomal instability and tumors promoted by DNA hypomethylation. *Science* 2003; **300**: 455.
34 Howard G, Eiges R, Gaudet F, Jaenisch R, Eden A. Activation and transposition of endogenous retroviral elements in hypomethylation induced tumors in mice. *Oncogene* 2008; **27**: 404–8.
35 Kitazawa S, Kitazawa R, Maeda S. Identification of methylated cytosine from archival formalin-fixed paraffin-embedded specimens. *Lab Invest* 2000; **80**: 275–6.
36 Hirohashi S, Ishak KG, Kojiro M *et al.* Hepatocellular carcinoma. In: Hamilton SR, Altonen LA, eds. *World Health Organization Classification of Tumours. Pathology and Genetics. Tumours of the Digestive System.* Lyon: IARC Press, 2000; 159–72.
37 Tsuda H, Zhang WD, Shimosato Y *et al.* Allele loss on chromosome 16 associated with progression of human hepatocellular carcinoma. *Proc Natl Acad Sci USA* 1990; **87**: 6791–4.
38 Kanai Y, Ushijima S, Tsuda H, Sakamoto M, Sugimura T, Hirohashi S. Aberrant DNA methylation on chromosome 16 is an early event in hepatocarcinogenesis. *Jpn J Cancer Res* 1996; **87**: 1210–17.

39 Takeichi M. Cadherin cell adhesion receptors as a morphogenetic regulator. *Science* 1991; **251**: 1451–5.

40 Oda T, Kanai Y, Oyama T *et al.* E-cadherin gene mutations in human gastric carcinoma cell lines. *Proc Natl Acad Sci USA* 1994; **91**: 1858–62.

41 Kanai Y, Oda T, Tsuda H, Ochiai A, Hirohashi S. Point mutation of the E-cadherin gene in invasive lobular carcinoma of the breast. *Jpn J Cancer Res* 1994; **85**: 1035–9.

42 Hirohashi S, Kanai Y. Cell adhesion system and human cancer morphogenesis. *Cancer Sci* 2003; **94**: 575–81.

43 Yoshiura K, Kanai Y, Ochiai A, Shimoyama Y, Sugimura T, Hirohashi S. Silencing of the E-cadherin invasion-suppressor gene by CpG methylation in human carcinomas. *Proc Natl Acad Sci USA* 1995; **92**: 7416–19.

44 Kanai Y, Ushijima S, Hui AM *et al.* The E-cadherin gene is silenced by CpG methylation in human hepatocellular carcinomas. *Int J Cancer* 1997; **71**: 355–9.

45 Wales MM, Biel MA, el Deiry W *et al.* p53 activates expression of HIC-1, a new candidate tumour suppressor gene on 17p13.3. *Nat Med* 1995; **1**: 570–77.

46 Chen WY, Zeng X, Carter MG *et al.* Heterozygous disruption of Hic1 predisposes mice to a gender-dependent spectrum of malignant tumors. *Nat Genet* 2003; **33**: 197–202.

47 Kanai Y, Hui AM, Sun L *et al.* DNA hypermethylation at the D17S5 locus and reduced HIC-1 mRNA expression are associated with hepatocarcinogenesis. *Hepatology* 1999; **29**: 703–9.

48 Kanai Y, Ushijima S, Ochiai A, Eguchi K, Hui A, Hirohashi S. DNA hypermethylation at the D17S5 locus is associated with gastric carcinogenesis. *Cancer Lett* 1998; **122**: 135–41.

49 Toyota M, Ahuja N, Ohe-Toyota M, Herman JG, Baylin SB, Issa JP. CpG island methylator phenotype in colorectal cancer. *Proc Natl Acad Sci USA* 1999; **96**: 8681–6.

50 Kanai Y, Ushijima S, Tsuda H, Sakamoto M, Hirohashi S. Aberrant DNA methylation precedes loss of heterozygosity on chromosome 16 in chronic hepatitis and liver cirrhosis. *Cancer Lett* 2000; **148**: 73–80.

51 Kondo Y, Kanai Y, Sakamoto M, Mizokami M, Ueda R, Hirohashi S. Genetic instability and aberrant DNA methylation in chronic hepatitis and cirrhosis: A comprehensive study of loss of heterozygosity and microsatellite instability at 39 loci and DNA hypermethylation on 8 CpG islands in microdissected specimens from patients with hepatocellular carcinoma. *Hepatology* 2000; **32**: 970–79.

52 Muller K, Heller H, Doerfler W. Foreign DNA integration. Genome-wide perturbations of methylation and transcription in the recipient genomes. *J Biol Chem* 2001; **276**: 14271–8.

53 Kondo Y, Kanai Y, Sakamoto M, Mizokami M, Ueda R, Hirohashi S. Microsatellite instability associated with hepatocarcinogenesis. *J Hepatol* 1999; **31**: 529–36.

54 Kanai Y, Ushijima S, Nakanishi Y, Sakamoto M, Hirohashi S. Mutation of the DNA methyltransferase (DNMT) 1 gene in human colorectal cancers. *Cancer Lett* 2003; **192**: 75–82.

55 Sun L, Hui AM, Kanai Y, Sakamoto M, Hirohashi S. Increased DNA methyltransferase expression is associated with an early stage of human hepatocarcinogenesis. *Jpn J Cancer Res* 1997; **88**: 1165–70.

56 Saito Y, Kanai Y, Sakamoto M, Saito H, Ishii H, Hirohashi S. Expression of mRNA for DNA methyltransferases and methyl-CpG-binding proteins and DNA methylation status on CpG islands and pericentromeric satellite regions during human hepatocarcinogenesis. *Hepatology* 2001; **33**: 561–8.

57 Saito Y, Kanai Y, Nakagawa T *et al.* Increased protein expression of DNA methyltransferase (DNMT) 1 is significantly correlated with the malignant potential and poor prognosis of human hepatocellular carcinomas. *Int J Cancer* 2003; **105**: 527–32.

58 Saito Y, Kanai Y, Sakamoto M, Saito H, Ishii H, Hirohashi S. Overexpression of a splice variant of DNA methyltransferase 3b, DNMT3b4, associated with DNA hypomethylation on pericentromeric satellite regions during human hepatocarcinogenesis. *Proc Natl Acad Sci USA* 2002; **99**: 10060–65.

59 Soejima K, Fang W, Rollins BJ. DNA methyltransferase 3b contributes to oncogenic transformation induced by SV40T antigen and activated Ras. *Oncogene* 2003; **22**: 4723–33.

60 Wong N, Lam WC, Lai PB, Pang E, Lau WY, Johnson PJ. Hypomethylation of chromosome 1 heterochromatin DNA correlates with q-arm copy gain in human hepatocellular carcinoma. *Am J Pathol* 2001; **159**: 465–71.

61 Kanai Y, Saito Y, Ushijima S, Hirohashi S. Alterations in gene expression associated with the overexpression of a splice variant of DNA methyltransferase 3b, DNMT3b4, during human hepatocarcinogenesis. *J Cancer Res Clin Oncol* 2004; **130**: 636–44.

62 Kanai Y, Ushijima S, Nakanishi Y, Hirohashi S. Reduced mRNA expression of the DNA demethylase, MBD2, in human colorectal and stomach cancers. *Biochem Biophys Res Commun* 1999; **264**: 962–6.

63 Etoh T, Kanai Y, Ushijima S *et al.* Increased DNA methyltransferase 1 (DNMT1) protein expression correlates significantly with poorer tumor differentiation and frequent DNA hypermethylation of multiple CpG islands in gastric cancers. *Am J Pathol* 2004; **164**: 689–99.

64 Kanai Y, Ushijima S, Kondo Y, Nakanishi Y, Hirohashi S. DNA methyltransferase expression and DNA methylation of CpG islands and peri-centromeric satellite regions in human colorectal and stomach cancers. *Int J Cancer* 2001; **91**: 205–12.

65 Issa JP. CpG island methylator phenotype in cancer. *Nat Rev Cancer* 2004; **4**: 988–93.

66 Tsai CL, Li HP, Lu YJ *et al.* Activation of DNA methyltransferase 1 by EBV LMP1 involves c-Jun NH(2)-terminal kinase signaling. *Cancer Res* 2006; **66**: 11668–76.

67 Maekita T, Nakazawa K, Mihara M *et al.* High levels of aberrant DNA methylation in Helicobacter pylori-infected gastric mucosae and its possible association with gastric cancer risk. *Clin Cancer Res* 2006; **12**: 989–95.

68 Sawada M, Kanai Y, Arai E, Ushijima S, Ojima H, Hirohashi S. Increased expression of DNA methyltransferase 1 (DNMT1) protein in uterine cervix squamous cell carcinoma and its precursor lesion. *Cancer Lett* 2007; **251**: 211–19.

69 Burgers WA, Blanchon L, Pradhan S, de Launoit Y, Kouzarides T, Fuks F. Viral oncoproteins target the DNA methyltransferases. *Oncogene* 2007; **26**: 1650–55.

70 Peng DF, Kanai Y, Sawada M *et al.* DNA methylation of multiple tumor-related genes in association with overexpression of DNA methyltransferase 1 (DNMT1) during multistage carcinogenesis of the pancreas. *Carcinogenesis* 2006; **27**: 1160–68.

71 Peng DF, Kanai Y, Sawada M *et al.* Increased DNA methyltransferase 1 (DNMT1) protein expression in precancerous conditions and ductal carcinomas of the pancreas. *Cancer Sci* 2005; **96**: 403–8.

72 Perwez Hussain S, Harris CC. Inflammation and cancer: An ancient link with novel potentials. *Int J Cancer* 2007; **121**: 2373–80.

73 Hodge DR, Peng B, Cherry JC *et al.* Interleukin 6 supports the maintenance of p53 tumor suppressor gene promoter methylation. *Cancer Res* 2005; **65**: 4673–82.

74 Baylin SB. Tying it all together: Epigenetics, genetics, cell cycle, and cancer. *Science* 1997; **277**: 1948–9.

75 Eguchi K, Kanai Y, Kobayashi K, Hirohashi S. DNA hypermethylation at the D17S5 locus in non-small cell lung cancers: Its association with smoking history. *Cancer Res* 1997; **57**: 4913–15.

76 Nakagawa T, Kanai Y, Saito Y, Kitamura T, Kakizoe T, Hirohashi S. Increased DNA methyltransferase 1 protein expression in human transitional cell carcinoma of the bladder. *J Urol* 2003; **170**: 2463–6.
77 Nakagawa T, Kanai Y, Ushijima S, Kitamura T, Kakizoe T, Hirohashi S. DNA hypermethylation on multiple CpG islands associated with increased DNA methyltransferase DNMT1 protein expression during multistage urothelial carcinogenesis. *J Urol* 2005; **173**: 1767–71.
78 Kakizoe T. Development and progression of urothelial carcinoma. *Cancer Sci* 2006; **97**: 821–8.
79 Nakagawa T, Kanai Y, Ushijima S, Kitamura T, Kakizoe T, Hirohashi S. DNA hypomethylation on pericentromeric satellite regions significantly correlates with loss of heterozygosity on chromosome 9 in urothelial carcinomas. *J Urol* 2005; **173**: 243–6.
80 Arai E, Kanai Y, Ushijima S, Fujimoto H, Mukai K, Hirohashi S. Regional DNA hypermethylation and DNA methyltransferase (DNMT) 1 protein overexpression in both renal tumors and corresponding nontumorous renal tissues. *Int J Cancer* 2006; **119**: 288–96.
81 Kanai Y, Ushijima S, Saito Y, Nakanishi Y, Sakamoto M, Hirohashi S. mRNA expression of genes altered by 5-azacytidine treatment in cancer cell lines is associated with clinicopathological parameters of human cancers. *J Cancer Res Clin Oncol* 2001; **127**: 697–706.
82 Hayashizaki Y, Hirotsune S, Okazaki Y *et al.* Restriction landmark genomic scanning method and its various applications. *Electrophoresis* 1993; **14**: 251–8.
83 Ushijima T, Morimura K, Hosoya Y *et al.* Establishment of methylation-sensitive-representational difference analysis and isolation of hypo- and hypermethylated genomic fragments in mouse liver tumors. *Proc Natl Acad Sci USA* 1997; **94**: 2284–9.
84 Toyota M, Ho C, Ahuja N *et al.* Identification of differentially methylated sequences in colorectal cancer by methylated CpG island amplification. *Cancer Res* 1999; **59**: 2307–12.
85 Shi H, Maier S, Nimmrich I *et al.* Oligonucleotide-based microarray for DNA methylation analysis: Principles and applications. *J Cell Biochem* 2003; **88**: 138–43.
86 Inazawa J, Inoue J, Imoto I. Comparative genomic hybridization (CGH)-arrays pave the way for identification of novel cancer-related genes. *Cancer Sci* 2004; **95**: 559–63.
87 Issa JP. DNA methylation as a therapeutic target in cancer. *Clin Cancer Res* 2007; **13**: 1634–7.

Genetic Clustering of Clear Cell Renal Cell Carcinoma Based on Array-Comparative Genomic Hybridization: Its Association with DNA Methylation Alteration and Patient Outcome

Eri Arai,[1] Saori Ushijima,[1] Hitoshi Tsuda,[6] Hiroyuki Fujimoto,[4] Fumie Hosoda,[2] Tatsuhiro Shibata,[2] Tadashi Kondo,[3] Issei Imoto,[5] Johji Inazawa,[5] Setsuo Hirohashi,[1] and Yae Kanai[1]

Abstract

Purpose: The aim of this study was to clarify genetic and epigenetic alterations occurring during renal carcinogenesis.

Experimental Design: Copy number alterations were examined by array-based comparative genomic hybridization analysis using an array harboring 4,361 bacterial artificial chromosome clones, and DNA methylation alterations on CpG islands of the *p16, human MutL homologue 1, von Hippel-Lindau*, and *thrombospondin 1* genes and the methylated in tumor (MINT-1, MINT-2, MINT-12, MINT-25, and MINT-31) clones were examined in 51 clear cell renal cell carcinomas (RCC).

Results: By unsupervised hierarchical clustering analysis based on copy number alterations, clear cell RCCs were clustered into the two subclasses, clusters A ($n = 34$) and B ($n = 17$). Copy number alterations were accumulated in cluster B. Loss of chromosome 3p and gain of 5q and 7 were frequent in both clusters A and B, whereas loss of 1p, 4, 9, 13q, and 14q was frequent only in cluster B. The average number of methylated CpG islands in cluster B was significantly higher than those in cluster A. Clear cell RCCs showing higher histologic grades, vascular involvement, renal vein tumor thrombi, and higher pathologic stages were accumulated in cluster B. The recurrence-free and overall survival rates of patients in cluster B were significantly lower than those of patients in cluster A. Multivariate analysis revealed that genetic clustering was a predictor of recurrence-free survival and was independent of histologic grade and pathologic stage.

Conclusions: This genetic clustering of clear cell RCC is significantly associated with regional DNA hypermethylation and may become a prognostic indicator for patients with RCC.

Renal cell carcinoma (RCC) is the most common malignant tumor of the adult kidney and frequently affects working-age adults in mid life (1). In general, RCCs at an early stage are curable by nephrectomy. However, some RCCs relapse and metastasize to distant organs, even if the resection has been considered complete. Metastatic RCCs are resistant to conventional chemotherapy and radiotherapy and have a poor outcome (2). Recently, immunotherapy has been established (3) and novel targeting agents have been developed (4) for treatment of RCC. However, unless relapsed or metastasized tumors are diagnosed early by close follow-up, the effectiveness of any therapy is very restricted. Therefore, to assist close follow-up of patients who have undergone nephrectomy and are still at risk of recurrence and metastasis, a prognostic indicator should be established based on an understanding of the molecular mechanisms of renal carcinogenesis.

Although the classification of RCC is based largely on histology, the WHO classification has introduced genetic alterations as a hallmark corresponding to the histologic subtypes of RCC, e.g., clear cell RCC, the most common histologic subtype, is characterized by loss of chromosome 3p and inactivation of the *von Hippel-Lindau* (*VHL*) gene at 3p25.3 (1). Somatic inactivation of the *VHL* gene occurs in only 60% to 70% of sporadic clear cell RCCs (5), and aberrations of the *VHL* gene alone cannot explain the development of all clear cell RCCs. However, only a few studies using recently developed array-based technology and demonstrating copy number alterations in clinical tissue samples of clear cell RCC have been reported (6, 7). In such previous array-based analyses, the numbers of examined clear cell RCCs and the numbers of clones on the arrays used were low, and significant prognostic factors for clear cell RCC based on array-based comparative

Authors' Affiliations: [1]Pathology Division, [2]Cancer Genomics Project, and [3]Proteome Bioinformatics Project, National Cancer Center Research Institute; [4]Urology Division, National Cancer Center Hospital; [5]Department of Molecular Cytogenetics, Medical Research Institute and School of Biomedical Science, Tokyo Medical and Dental University, Tokyo, Japan; and [6]Department of Pathology II, National Defense Medical College, Tokorozawa, Saitama, Japan

Received 2/21/08; revised 4/16/08; accepted 5/12/08.

Grant support: Grant-in-Aid for the Third-Term Comprehensive 10-Year Strategy for Cancer Control from the Ministry of Health, Labor and Welfare of Japan; Grant-in-Aid for Cancer Research from the Ministry of Health, Labor and Welfare of Japan; grant from the New Energy and Industrial Technology Development Organization; and Program for Promotion of Fundamental Studies in Health Sciences of the National Institute of Biomedical Innovation.

The costs of publication of this article were defrayed in part by the payment of page charges. This article must therefore be hereby marked *advertisement* in accordance with 18 U.S.C. Section 1734 solely to indicate this fact.

Requests for reprints: Yae Kanai, Pathology Division, National Cancer Center Research Institute, 5-1-1 Tsukiji, Chuo-ku, Tokyo 104-0045, Japan. Phone: 81-3-3542-2511; Fax: 81-3-3248-2463; E-mail: ykanai@ncc.go.jp.

doi:10.1158/1078-0432.CCR-08-0443

genomic hybridization (CGH) profiles have never been proposed.

We have reported that DNA methylation alterations are another important change occurring during renal carcinogenesis (8, 9). Accumulation of DNA methylation on C-type CpG islands in a cancer-specific but not age-dependent manner (10) in clear cell RCCs was significantly correlated with tumor aggressiveness and poorer patient outcome (8, 9). DNA methylation alterations were observed even in noncancerous renal tissues obtained from patients with clear cell RCCs, and such renal tissues were considered to be at the precancerous stage. Accumulation of DNA methylation on C-type CpG islands in such noncancerous renal tissues was significantly correlated with higher histologic grades of the corresponding clear cell RCCs developing in individual patients, suggesting that regional DNA hypermethylation in precancerous conditions generates more malignant RCCs (8, 9). However, to our knowledge, no published systematic reports have examined the correlation between copy number alterations and changes in DNA methylation. Therefore, current understanding of the genetic and epigenetic alterations occurring during renal carcinogenesis is far from complete.

In this study, we analyzed copy number alterations by array-CGH using a microarray of 4,361 bacterial artificial chromosome (BAC) clones, allowing high-resolution genome-wide analysis, and DNA methylation alterations on 9 CpG islands by bisulfite modification in 51 clear cell RCCs. Correlations between copy number alterations and changes in DNA methylation, and the clinicopathologic significance and prognostic effect of the copy number alterations, were examined.

Materials and Methods

Patients and tissue samples. Tumor tissues were obtained from materials surgically resected from 51 patients (RCC01 to RCC51) with primary clear cell RCC. These patients did not receive preoperative treatment and underwent nephrectomy at the National Cancer Center Hospital, Tokyo, Japan, between 1999 and 2006. There were 34 men and 17 women with a mean (±SD) age of 59 ± 10 years (range 31-81 years). Histologic diagnosis was made in accordance with the WHO classification (1). All the tumors were graded on the basis of previously described criteria (11) and classified according to the pathologic tumor-node-metastasis (TNM) classification (12). The presence or absence of vascular involvement was examined microscopically on slides stained with H&E and elastica van Gieson. The presence or absence of tumor thrombi in the main trunk of the renal vein was examined macroscopically. This study was approved by the Ethics Committee of the National Cancer Center, Tokyo, Japan.

Clear cell RCC is usually enclosed by a fibrous capsule and is well demarcated, hardly ever containing a fibrous stroma between the cancer cells. Therefore, we were able to obtain cancer cells of high purity from surgical specimens, avoiding contamination with both noncancerous epithelial cells and stromal cells. High-molecular-weight DNA from fresh frozen tumor samples was extracted with phenol-chloroform, followed by dialysis.

Array-CGH analysis. Copy number alterations were analyzed by array-CGH using a custom-made array (MCG Whole Genome Array-4500) harboring 4,361 BAC clones throughout chromosomes 1 to 22 and X and Y, providing a resolution of ~0.7 Mb (13), as described previously (14, 15). Briefly, gender-matched Human Genomic DNA (Promega) was used as reference. *Dpn*II-restricted test and reference genomic DNAs were labeled by random priming with Cy3- and Cy5-dCTP (GE Healthcare), respectively, using a BioPrime array CGH genomic labeling system (Invitrogen) and precipitated together with ethanol in the presence of Cot-I DNA. The mixture was applied to array slides and incubated at 43°C for 72 h. Arrays were scanned with a GenePix Personal 4100A (Axon Instruments) and analyzed using GenePix Pro 5.0 imaging software (Axon Instruments) and Acue 2 software (Mitsui Knowledge Industry).

The results of array-CGH were validated by fluorescence *in situ* hybridization (FISH) analysis in representative RCCs as described previously (16). BAC clones, RP11-115G3 (3p25.3), RP11-4E3 (5q31.1), and RP11-79I6 (5q32), which are included in the MCG Whole Genome Array-4500, were labeled with SpectrumOrange-dUTP (Abbott Laboratories) using a nick translation kit (Abbott Laboratories) and hybridized to 5-μm-thick sections of formalin-fixed, paraffin-embedded tissue specimens taken from a region immediately adjoining that from which the corresponding fresh frozen sample had been obtained within the same RCC. Nuclei were stained with 4,5-diamidino-2-phenylindole.

Methylation-specific PCR and combined bisulfite restriction enzyme analysis. DNA methylation status on 9 CpG islands (8 C-type CpG islands plus the CpG island of the *VHL* gene) was analyzed by methylation-specific PCR and combined bisulfite restriction enzyme analysis as described previously (17, 18). Briefly, bisulfite conversion was carried out using a CpGenome DNA Modification Kit (Chemicon International). DNA methylation status on CpG islands of the *p16, human MutL homologue 1* (*hMLH1*), and *VHL* genes was determined by methylation-specific PCR using the primers described previously (19, 20). The DNA methylation status of the *thrombospondin* (*THBS*) *1* gene and the methylated in tumor (MINT)-1, MINT-2, MINT-12, MINT-25, and MINT-31 clones was determined by combined bisulfite restriction enzyme analysis using previously described primers (10) and restriction enzymes (8).

Statistics. Unsupervised hierarchical clustering analysis of the RCCs was done using Impressionist software (Gene Data) as described previously (15, 21, 22). The average number of BAC clones for which copy number alterations (loss and gain) were observed in clear cell RCCs belonging to clusters A and B yielded by the unsupervised hierarchical clustering was analyzed using the Mann-Whitney *U* test. The frequency of copy number alterations (loss and gain) on each BAC clone, DNA methylation on each CpG island, and CpG island methylator phenotype in clusters A and B were analyzed using the χ^2 test. Correlations between genetic clustering of clear cell RCC (clusters A and B) and clinicopathologic variables were analyzed using the χ^2 test. Survival curves were calculated by the Kaplan-Meier method according to genetic clustering of clear cell RCC (clusters A and B), and the differences were analyzed by the log-rank test. The Cox proportional hazards multivariate model was used to examine the prognostic effect of genetic clustering of clear cell RCC (clusters A and B), histologic grade, and pathologic TNM stage. Differences with P values of <0.05 were considered significant.

Results

Array-CGH analysis. Examples of array-CGH profiles of the two representative clear cell RCCs (RCC01 and RCC02) are shown in Fig. 1A to D (Fig. 1A and B for RCC01 and Fig. 1C and D for RCC02). Fig. 1A and C are scattergrams of the signal ratios (test signal/reference signal) and Fig. 1B and D are the corresponding histograms. As shown in Fig. 1B and D, the histograms of the signal ratios showed multiple distinct peaks. The thresholds of the signal ratios for copy numbers 0, 1, 2, 3, and 4 or more were determined by the troughs between the peaks on the histogram of each RCC (*red bars*, Fig. 1B and D for RCC01 and RCC02, respectively). For example, the signal ratio of the RP11-115G3 clone in RCC01, shown as an asterisk in Fig. 1A and B, corresponded to copy number 1 (Fig. 1B).

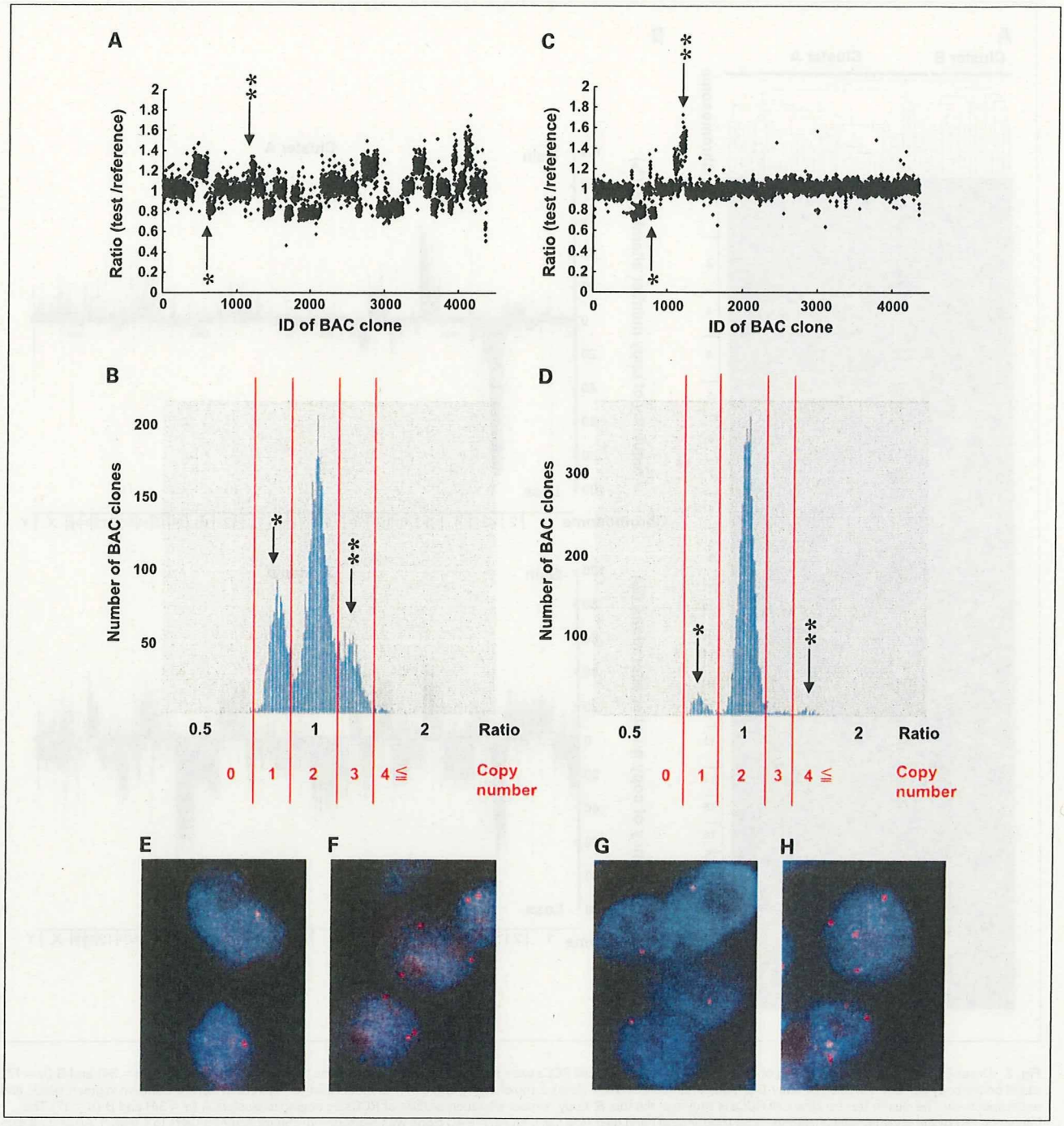

Fig. 1. Copy number alterations in two representative clear cell RCCs (RCC01 and RCC02) revealed by array-CGH and validated by FISH. The scattergrams (*A* and *C*) and the histograms (*B* and *D*) of the signal ratios (test signal/reference signal) afforded by array-CGH in RCC01 (*A* and *B*) and RCC02 (*C* and *D*). The thresholds of the signal ratios for copy numbers of 0, 1, 2, 3, and 4 or more were determined by the troughs (*red bars, B* and *D*) between the distinct peaks for RCC01 (*B*) and RCC02 (*D*). In RCC01, the signal ratios of clones RP11-115G3 (*, *A* and *B*) and RP11-4E3 (**, *A* and *B*) corresponded to copy numbers of 1 and 3, respectively (*B*). In RCC02, the signal ratios of clones RP11-115G3 (*, *C* and *D*) and RP11-4E3 (**, *C* and *D*) corresponded to copy numbers of 1 and 4 or more, respectively (*D*). FISH analysis using clones RP11-115G3 and RP11-4E3 as probes actually revealed 1 (*E*) and 3 (*F*) signals in RCC01, respectively. FISH analysis using clones RP11-115G3 and RP11-4E3 as probes actually revealed 1 (*G*) and 4 (*H*) signals in RCC02, respectively.

Similarly, the signal ratio of the RP11-4E3 clone in RCC01, shown as double asterisks in Fig. 1A and B, corresponded to copy number 3 (Fig. 1B). The signal ratios of the RP11-115G3 and RP11-4E3 clones in RCC02, shown as an asterisk and double asterisks in Fig. 1C and D, corresponded to copy numbers 1 and 4 or more, respectively (Fig. 1D). These data for copy numbers were validated by FISH analysis: clones RP11-115G3 and RP11-4E3 actually revealed 1 and 3 signals in

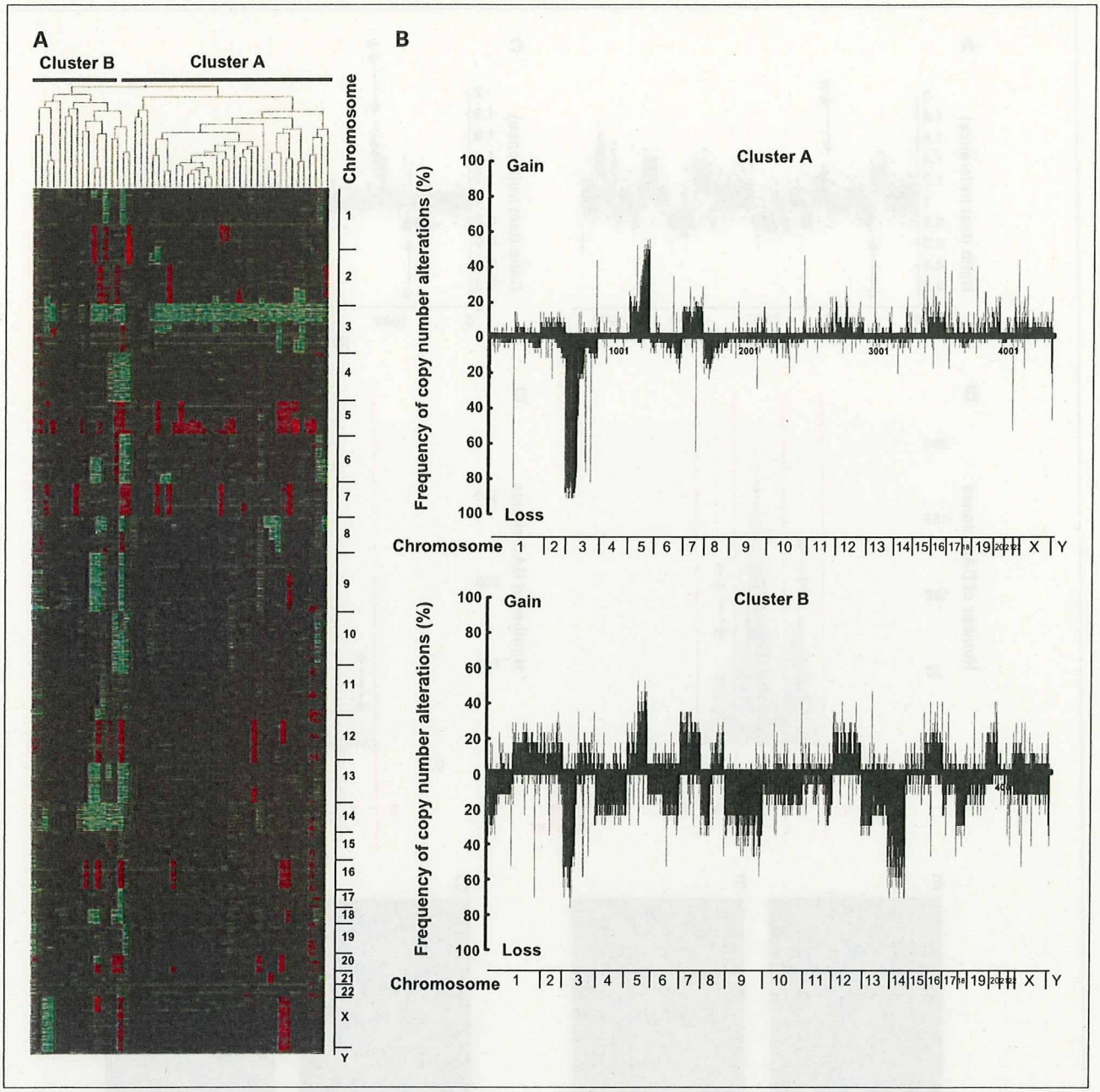

Fig. 2. Unsupervised hierarchical clustering of clear cell RCCs. *A,* 51 clear cell RCCs were hierarchically clustered into the two subclasses, clusters A (n = 34) and B (n = 17), based on the copy numbers revealed by array-CGH. Copy numbers of 0 or 1 (loss), 2 (no change), and 3 or 4 or more (gain) on each BAC clone are shown in green, black, and red, respectively. The cluster tree for clear cell RCCs is shown at the top. *B,* copy number alteration profiles of RCCs belonging to clusters A (n = 34) and B (n = 17). The frequency (%) of the copy number alterations, loss (*bottom half*) and gain (*top half*), on each BAC clone was plotted from chromosome 1p (*left*) to Y (*right*). Artifactual data due to copy number variants deposited in the databases described in ref. 32 are omitted from this figure. In both clusters, loss or gain of an entire chromosome or an entire chromosome arm was frequent. Loss of chromosome 3p and gain of chromosomes 5q and 7 were frequent in both clusters A and B. Loss of chromosomes 1p, 4, 9, 13q, and 14q was frequent only in cluster B but not in cluster A. Gain on 1q31-ter, 3q, and 8q was frequent only in cluster B, whereas loss on the same loci was observed in cluster A.

RCC01 (Fig. 1E and F, respectively) and clones RP11-115G3 and RP11-4E3 actually revealed 1 and 4 signals in RCC02 (Fig. 1G and H, respectively).

Unsupervised hierarchical clustering of clear cell RCC based on array-CGH data. By unsupervised hierarchical clustering analysis of the RCCs based on array-CGH data, 51 clear cell RCCs were clustered into the two subclasses, clusters A and B (Fig. 2A), which contained 34 and 17 clear cell RCCs, respectively.

The copy number on each BAC clone was defined as a loss, no change, and a gain when it was 0 or 1, 2, and 3 or 4 or more. In clear cell RCCs, the average number of BAC clones on which loss was detected was significantly higher in cluster B (563 ± 568) than in cluster A (164 ± 116, P = 0.0174). The average

number of BAC clones on which gain was detected tended to be higher in cluster B (319 ± 306) than in cluster A (206 ± 243). The average number of BAC clones on which loss or gain was detected was significantly higher in cluster B (881 ± 831) than in cluster A (370 ± 274, $P = 0.0368$), indicating that copy number alterations were significantly accumulated in cluster B compared with cluster A. Figure 2B shows the copy number alteration profiles of clusters A and B. In both clusters, loss or gain of an entire chromosome or an entire chromosome arm was frequent (Fig. 2B). Table 1 shows an overview of the copy number alterations in clusters A and B, and the frequency of loss and gain on a BAC clone, which represented the tendency for the entire chromosome arm, per chromosome arm.

Figure 2B shows that loss of chromosome 3p and gain of chromosomes 5q and 7 were frequent in both clusters A and B. These data are confirmed in Table 1: The frequency of loss on clone RP11-865O5 (3p14.3-3p21.1) in clusters A and B was high (91% and 76%, respectively) and there was no significant difference in the frequency between the clusters ($P = 0.3139$; Table 1). Similarly, the frequency of gain on clones RP11-125L2 (5q35.2), RP11-90J13 (7p14), and RP11-451M8 (7q11.22) in clusters A and B was high and there was no significant difference in the frequency between the clusters ($P = 0.7660$, $P = 0.2935$, $P = 0.1855$ for RP11-125L2, RP11-90J13, RP11-451M8 clones, respectively, Table 1). Figure 2B shows that loss of chromosomes 1p, 4, 9, 13q, and 14q was frequent only in cluster B, but not in cluster A. These data are confirmed in Table 1: The frequency of loss on clones RP11-4O6 (1p35.3), RP11-38M16 (4p12), RP11-11P20 (4q28.1), RP11-327L3 (9p13.1-9p13.3), RP11-65C15 (9q21.3-9q22.1),

Table 1. Copy number alterations on BAC clones that represented the tendency for the entire chromosome arm

BAC clone	Location	Chromosomal gain			Chromosomal loss		
		Cluster A	Cluster B	P*	Cluster A	Cluster B	P*
RP11-4O6	1p35.3	0 (0%)	0 (0%)		0 (0%)	5 (29%)	0.0047
RP11-196B7	1q25.3	2 (6%)	3 (18%)	0.4052	0 (0%)	0 (0%)	
RP11-135J2	1q41	0 (0%)	4 (24%)	0.0167	2 (6%)	0 (0%)	0.7987
RP11-87C16	2p12-2p13	4 (12%)	3 (18%)	0.8856	0 (0%)	0 (0%)	
RP11-79C24	2q34	3 (9%)	5 (29%)	0.1343	3 (9%)	1 (6%)	0.8539
RP11-865O5	3p14.3-3p21.1	0 (0%)	0 (0%)		31 (91%)	13 (76%)	0.3139
RP11-91B3	3q13.1	0 (0%)	3 (18%)	0.0583	8 (24%)	0 (0%)	0.0768
RP11-38M16	4p12	0 (0%)	0 (0%)		0 (0%)	5 (29%)	0.0047
RP11-11P20	4q28.1	0 (0%)	0 (0%)		0 (0%)	5 (29%)	0.0047
RP11-36H5	5p15.2	8 (24%)	5 (29%)	0.9096	0 (0%)	0 (0%)	
RP11-125L2	5q35.2	19 (56%)	8 (47%)	0.7660	0 (0%)	0 (0%)	
RP11-145L22	6p21.32-6p22.2	1 (3%)	1 (6%)	0.7987	0 (0%)	2 (12%)	0.2022
RP11-71B1	6q25.1-6q25.3	0 (0%)	0 (0%)		7 (21%)	6 (35%)	0.4265
RP11-90J13	7p14	6 (18%)	6 (35%)	0.2935	0 (0%)	0 (0%)	
RP11-451M8	7q11.22	5 (15%)	6 (35%)	0.1855	0 (0%)	0 (0%)	
RP11-277I21	8p12	0 (0%)	0 (0%)		8 (24%)	6 (35%)	0.5791
RP11-90N3	8q21.3-8q22	0 (0%)	5 (29%)	0.0047	2 (6%)	0 (0%)	0.7987
RP11-327L3	9p13.1-9p13.3	0 (0%)	0 (0%)		0 (0%)	7 (41%)	0.0003
RP11-65C15	9q21.3-9q22.1	1 (3%)	0 (0%)	0.7210	0 (0%)	8 (47%)	<0.0001
RP11-24J20	10p13-10p15.2	0 (0%)	0 (0%)		2 (6%)	3 (18%)	0.4052
RP11-178A10	10q11.21-10q11.23	0 (0%)	0 (0%)		3 (9%)	6 (35%)	0.0514
RP11-36H11	11p12-11p13	1 (3%)	1 (6%)	0.7987	0 (0%)	1 (6%)	0.7210
RP11-158I9	11q23	2 (6%)	0 (0%)	0.7987	0 (0%)	5 (29%)	0.0047
RP11-96K24	12p13.1	6 (18%)	6 (35%)	0.2935	0 (0%)	0 (0%)	
RP11-97N16	12q13.2-12q13.3	11 (32%)	9 (53%)	0.2647	0 (0%)	0 (0%)	
RP11-8C15	13q12.1	0 (0%)	0 (0%)		0 (0%)	6 (35%)	0.0013
RP11-140I4	14q32.1	0 (0%)	0 (0%)		0 (0%)	12 (71%)	<0.0001
RP11-265N6	15q15	1 (3%)	1 (6%)	0.7987	1 (3%)	1 (6%)	0.7987
RP11-295D4	16p13.3	7 (21%)	3 (18%)	0.9008	0 (0%)	1 (6%)	0.7210
RP11-48I18	16q11.2-16q12.1	8 (24%)	5 (29%)	0.9096	0 (0%)	0 (0%)	
RP11-89D11	17p13	2 (6%)	0 (0%)	0.7987	0 (0%)	4 (24%)	0.0167
RP11-89B11	17q25	2 (6%)	0 (0%)	0.7987	0 (0%)	3 (18%)	0.0583
RP11-106J7	18p11.31-18p11.32	1 (3%)	0 (0%)	0.7210	1 (3%)	8 (47%)	0.0005
RP11-12J12	18q21.32	1 (3%)	0 (0%)	0.7210	3 (9%)	7 (41%)	0.0178
RP11-201F4	19p13.2	1 (3%)	0 (0%)	0.7210	0 (0%)	3 (18%)	0.0583
RP11-133A7	19q13.2	0 (0%)	0 (0%)		0 (0%)	4 (24%)	0.0167
RP11-134G22	20p11.2-20p12	6 (18%)	4 (24%)	0.9008	0 (0%)	1 (6%)	0.7210
RP11-124D1	20q13.1	8 (24%)	7 (41%)	0.3281	0 (0%)	0 (0%)	
RP11-89H5	21q21.3	1 (3%)	2 (12%)	0.5279	1 (3%)	0 (0%)	0.7210
RP11-89J4	22q12	0 (0%)	1 (6%)	0.7210	1 (3%)	4 (24%)	0.0670
RP11-386N14	Xp11.23-Xp11.4	1 (3%)	2 (12%)	0.5279	1 (3%)	4 (24%)	0.0670
RP11-449M9	Xq13.1-Xq13.3	3 (9%)	1 (6%)	0.8539	0 (0%)	4 (24%)	0.0167
RP11-115H13	Yp11.31	2 (6%)	4 (24%)	0.1667	6 (18%)	5 (29%)	0.5473
RP11-88F4	Yq12	8 (24%)	1 (6%)	0.2425	6 (18%)	4 (24%)	0.9008

NOTE: P values <0.05, which indicate significant differences, are underlined.
*χ^2 test.

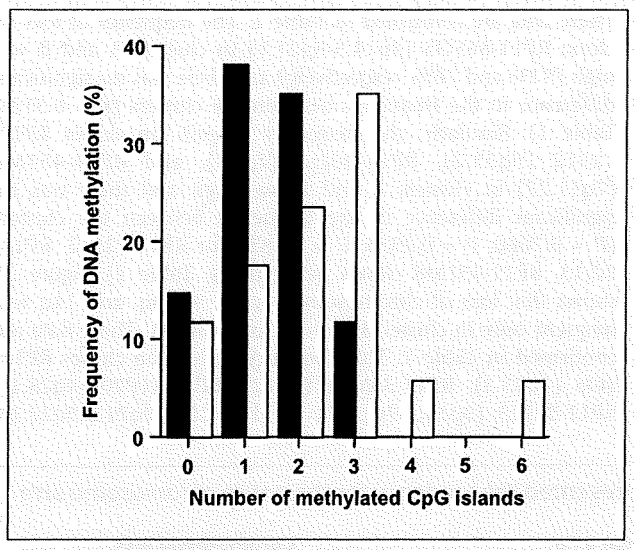

Fig. 3. Histogram showing the number of methylated CpG islands in RCCs belonging to clusters A (n = 34, *black column*) and B (n = 17, *white column*). DNA methylation on CpG islands was accumulated in cluster B compared with cluster A, and DNA methylation on 4 or more CpG islands was observed only in cluster B and never in cluster A.

RP11-8C15 (13q12.1), and RP11-140I4 (14q32.1) in cluster B (29%, 29%, 29%, 41%, 47%, 35%, and 71%) was significantly (P = 0.0047, P = 0.0047, P = 0.0047, P = 0.0003, P < 0.0001, P = 0.0013 and P < 0.0001) higher than that in cluster A (0%, 0%, 0%, 0%, 0%, 0%, and 0%, respectively, Table 1). Figure 2B shows that gain on 1q31-ter, 3q, and 8q was frequent only in cluster B, whereas loss at the same loci was observed in cluster A. These data are confirmed in Table 1: The frequency of gain on clones RP11-135J2 (1q41), RP11-91B3 (3q13.1), and RP11-90N3 (8q21.3-8q22) in cluster B was 24%, 18%, and 29%, whereas that in cluster A was 0%, 0%, and 0% and the frequency of loss on the same clones in cluster A was 6%, 24%, and 6%, respectively (Table 1).

Correlation between genetic clustering of clear cell RCC and accumulation of DNA methylation on CpG islands. DNA methylation status on the nine CpG islands in 41 clear cell RCCs of the present cohort had been already analyzed and was included in our previous article (8). DNA methylation status in the remaining 10 clear cell RCCs was analyzed here. The frequency of DNA methylation on CpG islands of the *p16*, *hMLH1*, *VHL*, and *THBS1* genes and the MINT-1, MINT-2, MINT-12, MINT-25, and MINT-31 clones was 23 of 34 (detected/analyzed, 68%), 4 of 34 (12%), 0 of 34 (0%), 5 of 34 (15%), 2 of 34 (6%), 0 of 34 (0%), 5 of 34 (15%), 10 of 34 (29%), and 0 of 34 (0%) in cluster A and 9 of 17 (53%), 1 of 17 (6%), 2 of 17 (12%), 10 of 17 (59%), 5 of 17 (29%), 2 of 17 (12%), 1 of 17 (6%), 9 of 17 (53%), and 0 of 17 (0%) in cluster B, respectively. The frequency of DNA methylation on CpG islands of the *THBS1* gene in cluster B was significantly higher than that in cluster A (P = 0.0034). The average number of methylated CpG islands was significantly higher in cluster B (2.29 ± 1.49) than in cluster A (1.44 ± 0.89, P = 0.0279). Patients were considered CpG island methylator phenotype–positive when DNA methylation was seen on three or more examined CpG islands, based on previously described criteria (10). The frequency of CpG island methylator phenotype in cluster B (47%) was significantly higher than that in cluster A (12%, P = 0.0142). Figure 3 shows a histogram of the number of methylated CpG islands in clusters A and B. DNA methylation on CpG islands was accumulated in cluster B compared with cluster A, and DNA methylation on 4 or more CpG islands was observed only in cluster B and never in cluster A (Fig. 3).

Clinicopathologic significance and prognostic effect of genetic clustering of clear cell RCC. Table 2 shows the clinicopathologic variables of clear cell RCCs belonging to clusters A and B. Clear cell RCCs in cluster B showed significantly higher histologic grades (P = 0.0063) and more frequently showed vascular involvement (P = 0.0045), renal vein tumor thrombi (P = 0.0064), and higher pathologic TNM stages (P = 0.0066) than those in cluster A (Table 2). Figure 4 shows the Kaplan-Meier survival curves of patients based on genetic clustering of clear cell RCC (clusters A and B). The period covered ranged from 88 to 2,801 days (mean, 1,679 days). After nephrectomy, none of the patients received any adjuvant therapy before recurrence or metastasis was revealed. Recurrence or metastasis was observed in 6 (40%) of 15 patients who underwent curative resection in cluster B, but in only 3 (9%) of 34 patients who underwent curative resection in cluster A. The recurrence-free survival rate of patients in cluster B was significantly lower than that of patients in cluster A (Fig. 4A; P = 0.0018). Four (24%) of the total 17 patients in cluster B died as a result, whereas none (0%) of the patients in cluster A died. The overall survival rate of patients in cluster B was significantly lower than that of patients in cluster A (Fig. 4B; P = 0.0009). Multivariate analysis revealed that genetic clustering was a predictor of recurrence-free survival (P = 0.0297) and was independent of

Table 2. Correlation between genetic clustering of clear cell RCC (clusters A and B) and clinicopathologic variables

Clinicopathologic variables	Genetic clustering		P
	Cluster A (n = 34)	Cluster B (n = 17)	
Size, cm (mean ± SD)	4.9 ± 2.5	6.3 ± 3.3	0.144*
Histologic grade			
Grade 1	25	8	0.0063†
Grade 2	8	3	
Grade 3	1	3	
Grade 4	0	3	
Vascular involvement‡			
Negative	30	8	0.0045†
Positive	4	9	
Renal vein tumor thrombi§			
Negative	32	10	0.0064†
Positive	2	7	
Pathologic TNM stage			
Stage I	24	5	0.0066†
Stage II	1	0	
Stage III	9	7	
Stage IV	0	5	

*Mann-Whitney U test.
† χ^2 test.
‡ Recognized microscopically on slides stained with H&E and elastica van Gieson.
§ Recognized macroscopically in the main trunk of the renal vein.

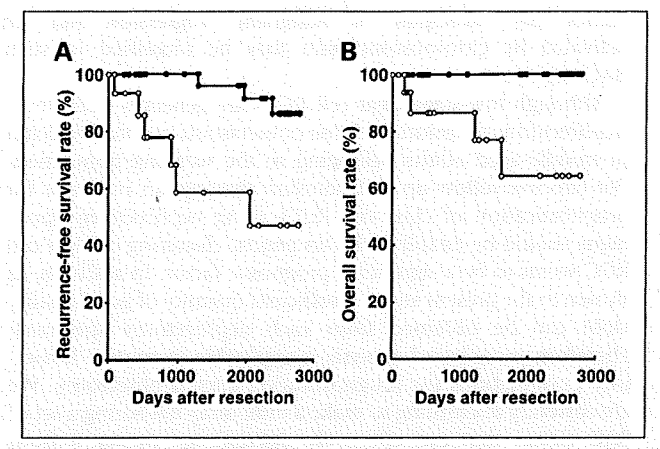

Fig. 4. Kaplan-Meier survival curves based on genetic clustering of clear cell RCC (clusters A and B). *A*, the recurrence-free survival rate of patients in cluster B (○) was significantly lower than that of patients in cluster A (●, $P = 0.0018$, log-rank test). *B*, none of the patients in cluster A (●) died as a result, and the overall survival rate of patients in cluster B (○) was significantly lower than that of patients in cluster A ($P = 0.0009$, log-rank test).

histologic grade and pathologic TNM stage (Table 3), although the effects of these three variables on overall survival were not independent from each other (data not shown).

Discussion

Only a few studies using recently developed array-based technology and demonstrating copy number alterations in clinical samples of clear cell RCCs have been reported (6, 7). Therefore, the genetic pathway of renal carcinogenesis has not been fully clarified. To our knowledge, the resolution achieved in the present study was higher than that of any other previous array-CGH analyses (6, 7) of clear cell RCCs. We used MCG Whole Genome Array-4500, which harbors 4361 BAC clones distributed throughout the human genome and has successfully revealed copy number alteration profiles in human cancers derived from various organs (13). Our array-CGH analysis was performed using RCC cells of high purity from fresh good-quality specimens and the results were carefully validated by FISH using the same BAC clones as probes.

First, our genome-wide analysis revealed that loss or gain of an entire chromosome or an entire chromosome arm was frequent in clear cell RCCs. Other than the well-studied *VHL* gene (3p25.3), some tumor-related genes may be identified in BAC regions where copy number alterations were observed. Unsupervised hierarchical clustering analysis based on array-CGH data grouped the 51 clear cell RCCs into two subclasses, clusters A and B, and copy number alterations were found to be significantly accumulated in cluster B. Moreover, we identified distinct copy number alteration profiles in the two clusters: (*a*) loss of chromosome 3p and gain of chromosomes 5q and 7 were frequent in both clusters A and B; (*b*) loss of chromosomes 1p, 4, 9, 13q, and 14q was frequent only in cluster B but not in cluster A; and (*c*) gain on 1q31-ter, 3q, and 8q was frequent only in cluster B, whereas loss on the same loci was observed in cluster A, although the frequency was rather low. Therefore, our clusters A and B, by unsupervised hierarchical clustering analysis, can be considered valid. Although the genetic profiles of clear cell RCCs obtained by CGH (23–25) and FISH (25–27) analyses without array-based technology have been compared with those of other histologic types of RCC (such as papillary RCC and chromophobe RCC), the subclasses of clear cell RCC itself, which may reflect the distinct genetic pathways of carcinogenesis, have not been defined. The present high-resolution, genome-wide analysis indicated that loss of chromosome 3p and gain of 5q and 7 may be indispensable copy number aberrations for the development of clear cell RCCs, regardless of genetic clustering. Additional loss of chromosomes 1p, 4, 9, 13q, and 14q may promote the genetic pathway to cluster B, although the order of occurrence of indispensable copy number aberrations and additional losses for cluster B during renal carcinogenesis has not yet been defined.

We have reported that DNA methylation alterations are an important epigenetic change during renal carcinogenesis (8, 9) and are significantly correlated with tumor aggressiveness and poorer patient outcome. However, to our knowledge, there have been no published systematic reports about the correlation between copy number alterations and DNA methylation alterations in clear cell RCCs. We therefore examined the correlation between array-CGH data and DNA methylation status. DNA methylation on CpG islands was accumulated in clear cell RCCs belonging to cluster B. The histogram of the number of methylated CpG islands (Fig. 3) revealed a tendency for biphasic accumulation only in cluster B, whereas a monophasic peak was observed in cluster A, and DNA methylation on 6 CpG islands, which corresponded to the second peak indicating severe accumulation, was detected only in cluster B. These data suggest that genetic and epigenetic alterations were not mutually exclusive during renal carcinogenesis and that our genetic clustering of clear cell RCC based on copy number alterations is significantly correlated with DNA methylation alterations. In cluster B, showing simultaneous accumulation of both copy number and DNA methylation alterations, tumor suppressor genes may be effectively silenced by a combination of chromosome loss and DNA hypermethylation on CpG islands. Genes that participate in chromosome integrity may be silenced by regional DNA hypermethylation. Such mechanisms linking genetic and epigenetic alterations should be further examined, especially in clear cell RCCs belonging to cluster B.

Finally, we examined the clinicopathologic significance and prognostic effect of our genetic clustering of clear cell RCC.

Table 3. Multivariate analysis of histologic grade and pathologic TNM stage and genetic clustering as predictors of recurrence-free survival

Variables	Hazard ratio (95% CI)	χ^2	*P*
Histologic grade			
Grade 1	1 (Reference)	2.312	0.1284
Grade 2, 3, or 4	3.291 (0.709-15.285)		
Pathologic TNM stage			
Stage I	1 (Reference)	1.662	0.1973
Stage II, III, or IV	3.214 (0.545-18.964)		
Genetic clustering			
Cluster A	1 (Reference)	4.724	0.0297
Cluster B	5.252 (1.177-23.442)		

Abbreviation: 95% CI, 95% confidence interval.

Clear cell RCCs showing higher histologic grades, vascular involvement, renal vein tumor thrombi, and higher pathologic TNM stages were accumulated in cluster B. Because there was no significant difference of tumor size between clusters A and B, it was not feasible for clear cell RCCs in cluster B to have simply been in existence longer than those in cluster A: genetic and epigenetic alterations in cluster B may not simply accumulate at the same constant speed as those in cluster A. Although it has been reported that careful dissection of large clear cell RCCs almost always reveals renal vein tumor thrombi (28), because there was no significant difference in tumor size between clusters A and B, accumulation of clear cell RCCs with renal vein tumor thrombi in cluster B was not attributable to the difference in tumor size. Recurrence-free and overall survival rates were significantly lower in cluster B patients than in cluster A patients. Previous studies using FISH (29) and microsatellite loss of heterozygosity (30) analyses and focusing on chromosome 9p have revealed that loss of 9p is associated with tumor recurrence and poorer outcome. A previous study that used the inter-Alu long PCR method focusing on chromosome 14q showed that loss of 14q was associated with poorer outcome (31). These separately examined variables are consistent with our results because loss of chromosomes 9 and 14q was frequent in cluster B. Our data suggest that our genetic clustering of clear cell RCC based on copy number alterations is significantly correlated with tumor aggressiveness and is a significant prognostic indicator. Accumulated genetic and epigenetic alterations may play a significant role in the malignant potential of clear cell RCCs belonging to cluster B. Multivariate analysis revealed that genetic clustering was a predictor of recurrence-free survival and was independent of histologic grade and pathologic TNM stage. Gain at some BAC clones on chromosomes 3q and 8q was observed only in clear cell RCCs showing recurrence. Genes that participate in malignant progression and are activated by chromosome gain may be identified in such BAC regions.

Although low-stage clear cell RCCs are generally curable by nephrectomy, occasional relapse or metastasis can lead to death in middle-aged adults belonging to the working population. For effective follow-up and adjuvant therapy, an indicator for prognostication of clear cell RCCs using nephrectomy specimens should be established. Our genetic clustering of clear cell RCC seems to be a significant prognostic factor. In addition, as shown in the present study, a sufficient quantity of good quality DNA can be obtained from each nephrectomy specimen. Therefore, array-based analysis is applicable to routine laboratory examinations for prognostication after nephrectomy. We are currently attempting to make a mini-array harboring a set of BAC clones that can effectively discriminate cluster B from cluster A for prognostication of clear cell RCCs. The reliability of such prognostication will need to be validated in a prospective study.

In summary, indispensable copy number aberrations, loss of chromosome 3p and gain of chromosomes 5q and 7, may solely promote the development of RCCs belonging to cluster A, which show a favorable outcome. When loss of chromosomes 1p, 4, 9, 13q, and 14q and DNA methylation alterations are added to loss of 3p and gain of 5q and 7, more malignant RCCs belonging to cluster B may develop. The order of occurrence of each genetic and epigenetic event during renal carcinogenesis has not yet been defined. Our genetic clustering associated with regional DNA hypermethylation may also become a prognostic indicator for clear cell RCCs.

Disclosure of Potential Conflicts of Interest

No potential conflicts of interest were disclosed.

References

1. Eble JN, Sauter G, Epstein JI, Sesterhenn IA. World Health Organization classification of tumours. Pathology and genetics. Tumours of the urinary system and male genital organs. Lyon: IARC Press; 2004. pp.10–43.
2. Jones J, Libermann TA. Genomics of renal cell cancer: the biology behind and the therapy ahead. Clin Cancer Res 2007;13:685–92s.
3. Guida M, Colucci G. Immunotherapy for metastatic renal cell carcinoma: is it a therapeutic option yet? Ann Oncol 2007;18:149–52.
4. Patel PH, Chadalavada RS, Chaganti RS, Motzer RJ. Targeting von Hippel-Lindau pathway in renal cell carcinoma. Clin Cancer Res 2006;12:7215–20.
5. Kondo K, Yao M, Yoshida M, et al. Comprehensive mutational analysis of the VHL gene in sporadic renal cell carcinoma: relationship to clinicopathological parameters. Genes Chromosomes Cancer 2002;34:58–68.
6. Wilhelm M, Veltman JA, Olshen AB, et al. Array-based comparative genomic hybridization for the differential diagnosis of renal cell cancer. Cancer Res 2002;62:957–60.
7. Yoshimoto T, Matsuura K, Karnan S, et al. High-resolution analysis of DNA copy number alterations and gene expression in renal clear cell carcinoma. J Pathol 2007;213:392–401.
8. Arai E, Kanai Y, Ushijima S, Fujimoto H, Mukai K, Hirohashi S. Regional DNA hypermethylation and DNA methyltransferase (DNMT) 1 protein overexpression in both renal tumors and corresponding nontumorous renal tissues. Int J Cancer 2006;119:288–96.
9. Kanai Y, Hirohashi S. Alterations of DNA methylation associated with abnormalities of DNA methyltransferases in human cancers during transition from a precancerous to a malignant state. Carcinogenesis 2007;28:2434–42.
10. Toyota M, Ahuja N, Ohe-Toyota M, Herman JG, Baylin SB, Issa JP. CpG island methylator phenotype in colorectal cancer. Proc Natl Acad Sci U S A 1999;96:8681–6.
11. Fuhrman SA, Lasky LC, Limas C. Prognostic significance of morphologic parameters in renal cell carcinoma. Am J Surg Pathol 1982;6:655–63.
12. Sobin LH, Wittekind Ch. International Union Against Cancer (UICC). TNM classification of malignant tumors, 6th ed. New York: Wiley-Liss; 2002. p.193–5.
13. Inazawa J, Inoue J, Imoto I. Comparative genomic hybridization (CGH)-arrays pave the way for identification of novel cancer-related genes. Cancer Sci 2004;95:559–63.
14. Sonoda I, Imoto I, Inoue J, et al. Frequent silencing of low density lipoprotein receptor-related protein 1B (LRP1B) expression by genetic and epigenetic mechanisms in esophageal squamous cell carcinoma. Cancer Res 2004;64:3741–7.
15. Shibata T, Uryu S, Kokubu A, et al. Genetic classification of lung adenocarcinoma based on array-based comparative genomic hybridization analysis: its association with clinicopathologic features. Clin Cancer Res 2005;11:6177–85.
16. Tsuda H. HER-2 (c-erbB-2) test update: present status and problems. Breast Cancer 2006;13:236–48.
17. Kanai Y, Ushijima S, Kondo Y, Nakanishi Y, Hirohashi S. DNA methyltransferase expression and DNA methylation of CpG islands and peri-centromeric satellite regions in human colorectal and stomach cancers. Int J Cancer 2001;91:205–12.
18. Etoh T, Kanai Y, Ushijima S, et al. Increased DNA methyltransferase 1 (DNMT1) protein expression correlates significantly with poorer tumor differentiation and frequent DNA hypermethylation of multiple CpG islands in gastric cancers. Am J Pathol 2004;164:689–99.
19. Herman JG, Graff JR, Myohanen S, Nelkin BD, Baylin SB. Methylation-specific PCR: a novel PCR assay for methylation status of CpG islands. Proc Natl Acad Sci U S A 1996;93:9821–6.
20. Herman JG, Umar A, Polyak K, et al. Incidence and functional consequences of hMLH1 promoter hypermethylation in colorectal carcinoma. Proc Natl Acad Sci U S A 1998;95:6870–5.
21. Yokoo H, Kondo T, Fujii K, Yamada T, Todo S, Hirohashi S. Proteomic signature corresponding to α fetoprotein expression in liver cancer cells. Hepatology 2004;40:609–17.
22. Seike M, Kondo T, Fujii K, et al. Proteomic signature of human cancer cells. Proteomics 2004;4:2776–88.
23. Junker K, Weirich G, Amin MB, Moravek P, Hindermann W, Schubert J. Genetic subtyping of renal cell carcinoma by comparative genomic hybridization. Recent Results Cancer Res 2003;162:169–75.
24. Alimov A, Sundelin B, Bergerheim U, et al. Molecular cytogenetic characterization shows higher genetic homogeneity in conventional renal cell carcinoma

compared to other kidney cancers. Int J Oncol 2004; 25:955–60.
25. Sanjmyatav J, Schubert J, Junker K. Comparative study of renal cell carcinoma by CGH, multicolor-FISH and conventional cytogenic banding analysis. Oncol Rep 2005;14:1183–7.
26. Receveur AO, Couturier J, Molinie V, et al. Characterization of quantitative chromosomal abnormalities in renal cell carcinomas by interphase four-color fluorescence *in situ* hybridization. Cancer Genet Cytogenet 2005;158:110–8.
27. Barocas DA, Mathew S, DelPizzo JJ, et al. Renal cell carcinoma sub-typing by histopathology and fluorescence *in situ* hybridization on a needle-biopsy specimen. BJU Int 2007;99:290–5.
28. Bonsib SM. T2 clear cell renal cell carcinoma is a rare entity: a study of 120 clear cell renal cell carcinomas. J Urol 2005;174:1199–202.
29. Brunelli M, EccherA, Gobbo S, et al. Loss of chromosome 9p is an independent prognostic factor in patients with clear cell renal cell carcinoma. Mod Pathol 2008;21:1–6.
30. Presti JC, Jr., Wilhelm M, Reuter V, Russo P, Motzer R, Waldman F. Allelic loss on chromosomes 8 and 9 correlates with clinical outcome in locally advanced clear cell carcinoma of the kidney. J Urol 2002;167: 1464–8.
31. Kaku H, Ito S, Ebara S, et al. Positive correlation between allelic loss at chromosome 14q24-31 and poor prognosis of patients with renal cell carcinoma. Urology 2004;64:176–81.
32. Feuk L, Carson AR, Scherer SW. Structural variation in the human genome. Nat Rev Genet 2006;7:85–97.

Minimally Invasive Intraductal Papillary-mucinous Carcinoma of the Pancreas: Clinicopathologic Study of 104 Intraductal Papillary-mucinous Neoplasms

Satoshi Nara, MD, Kazuaki Shimada, MD, PhD,† Tomoo Kosuge, MD, PhD,† Yae Kanai, MD, PhD,* and Nobuyoshi Hiraoka, MD, PhD**

Abstract: Invasive intraductal papillary-mucinous carcinoma (I-IPMC) is a heterogeneous entity with various postoperative outcomes. The aim of this study is to characterize early-stage I-IPMC with nonaggressive characteristics. One hundred and four patients with intraductal papillary-mucinous neoplasm (IPMN) were clinicopathologically investigated. The lesions were classified into 53 noninvasive IPMNs (adenoma, borderline, and noninvasive IPMC) and 51 I-IPMCs on the basis of the WHO classification. I-IPMCs were divided further into 26 minimally invasive IPMCs (MI-IPMCs) and 25 invasive carcinomas originating in IPMC (IC-IPMCs) by new diagnostic criteria proposed in this study. We examined invasiveness of I-IPMC on 4 patterns, and defined simple and practical diagnostic criteria of minimal invasion for each invasive pattern. The disease-specific survival rates after 3, 5, and 10 years were 100%, 100%, and 100% for both noninvasive IPMN and MI-IPMC, and 51%, 38%, and 0% for IC-IPMC. The overall and disease-specific survival rates for MI-IPMC were both significantly better than those for IC-IPMC ($P < 0.001$), but there was no significant difference between noninvasive IPMN and MI-IPMC. Multivariate analysis showed that the factors indicative of poor prognosis were a diagnosis of I-IPMC classified as IC-IPMC and a high level of serum carbohydrate antigen 19-9. The prognosis of IC-IPMC was not significantly different from that of pancreatic ductal carcinoma in each of the corresponding tumor-node-metastasis stages. These findings suggest that a category of MI-IPMC provides more accurate and useful information of the stage and the aggressiveness of I-IPMC.

Key Words: intraductal papillary-mucinous neoplasms of the pancreas, minimal invasion, prognosis, clinicopathologic analysis, invasive pattern

(*Am J Surg Pathol* 2008;32:243–255)

From the *Pathology Division, National Cancer Center Research Institute; and †Division of Hepato-Biliary and Pancreatic Surgery, National Cancer Center Hospital, Tokyo.

Supported by a Grant-in-Aid for Third Term Comprehensive 10-year Strategy for Cancer Control from the Ministry of Health, Labor and Welfare of Japan and a Grant-in-Aid for Scientific Research from the Ministry of Education, Culture, Sports, Science and Technology of Japan. The authors have no direct or indirect commercial and financial incentive associated with publishing the article.

Reprints: Nobuyoshi Hiraoka, MD, PhD, Pathology Division, National Cancer Center Research Institute, 5-1-1 Tsukiji, Chuo-ku, Tokyo 104-0045, Japan (e-mail: nhiraoka@gan2.res.ncc.go.jp).

Intraductal papillary-mucinous neoplasm (IPMN) of the pancreas is a well-characterized clinical and pathologic entity. IPMNs are characterized by intraductal proliferation of neoplastic mucinous cells, which usually form papillae and lead to cystic dilation of the pancreatic ducts, forming clinically and macroscopically detectable masses.[15] Similarly to the well-defined adenoma-carcinoma sequence in colorectal cancer,[5] IPMNs progress from intraductal papillary-mucinous adenoma (IPMA) to borderline IPMN, then to intraductal papillary-mucinous carcinoma (IPMC), and eventually to invasive adenocarcinoma.[2,9,10] According to the WHO classification,[13,15] IPMC is classified as either "noninvasive" or "invasive." It is reported that noninvasive IPMN shows a favorable postoperative outcome in comparison with invasive IPMC (I-IPMC), with 5-year survival rates ranging from 77% to 100%.[4,6,16,20,22,24] With regard to the prognosis of I-IPMC, there is a substantial variation in the 5-year survival rates from 24% to 60% in previous reports.[4,6,16,20,22–24] This may be due to heterogeneity of I-IPMCs, including an invasive component of various sizes and biologic behavior. Our hypothesis is that the prognosis of I-IPMC can be substantially determined by the degree and type of invasion, and thus I-IPMC can be classified as either aggressive or nonaggressive by categorization according to the extent and pattern of invasion. Such a classification would be clinically relevant for deciding whether surgery is indicated, for selecting the most appropriate surgical procedure, and for prediction of postoperative outcome.

The concept of minimally invasive cancer was originally introduced for uterine cervical cancer showing very early invasion and a favorable prognosis.[26] Minimally invasive IPMC (MI-IPMC) has been categorized within the classification of pancreatic carcinoma used by the Japan Pancreatic Society (JPS) since 1993.[12] In the JPS classification, I-IPMC is classified into 2 categories: MI-IPMC and invasive carcinoma originating in IPMC (IC-IPMC), the latter being more advanced. A few reports have indicated that MI-IPMC has a better surgical outcome than IC-IPMC.[19,25,27] However, the definition of "minimal invasion" has not been clear. In the original JPS text, it is described only as "slight invasion beyond the pancreatic duct wall."[12]

In this retrospective study, we evaluated the invasiveness of I-IPMC by the examination of 4 invasive

patterns, and tried to define simple and practical diagnostic criteria of minimal invasion for each invasive pattern. The clinical relevance of this subdivision was then evaluated in terms of postoperative survival.

MATERIALS AND METHODS

Study Population

This study was approved by the Ethics Committee of the National Cancer Center, Japan. Between January 1984 and December 2005, 111 patients underwent pancreatic resection for IPMNs at the National Cancer Center Hospital, Japan. There were no operation-related deaths, and all patients underwent macroscopically curative resection without any residual tumor. Seven cases also had ductal carcinoma of the pancreas, which was not directly associated with IPMNs. Excluding these patients, 104 cases of IPMN were included in this study. The patients comprised of 56 males and 48 females with a median age of 66 (41 to 84) years. The operative procedures included 12 pancreatoduodenectomies (PDs), 59 pylorus-preserving PDs (PPPDs), 24 distal pancreatectomies, 3 total pancreatectomies, 5 partial pancreatectomies, and 1 PPPD with distal pancreatectomy. These procedures accounted for 18.9% of all pancreatectomies (n = 551) performed at our institution for pancreatic tumors during the same period.

Every patient was followed up in the outpatient clinic every 1 to 3 months during the first postoperative year, and every 6 to 12 months thereafter. No patient dropped out during follow-up. Clinical or radiologic data and follow-up information for every patient were obtained from the medical records. The median follow-up period after surgery was 37.2 (4.2 to 210) months for all patients, 52.9 (4.2 to 171) months for noninvasive IPMN, 43.4 (13.2 to 210) months for MI-IPMC, and 20.4 (7.1 to 87.7) months for IC-IPMC.

Pathologic Examination

All of the IPMNs were pathologically reexamined and the diagnosis of IPMN was confirmed. Surgically resected specimens were fixed in 10% formalin and cut into serial 5-mm-thick slices, horizontally in the pancreas head, and sagittally in the pancreas body and tail. All the sections were stained with hematoxylin and eosin for pathologic examination. If necessary, additional staining for elastic fibers (elastica stain) was performed. After histopathologic examination of all the sections, the lesion was classified as IPMA, borderline IPMN, noninvasive IPMC, or I-IPMC according to the WHO classification.[13,15] The lesion was graded by the highest degree of atypia. I-IPMCs were divided further into MI-IPMC or IC-IPMC according to our proposed criteria (Table 1) described later. We evaluated the invasiveness of I-IPMC, and the 4 invasive patterns were examined: "infiltrative growth," "mucous rupture," "expansive growth," and "intra-abdominal rupture." The criterion of minimal invasion was proposed for each invasive pattern. I-IPMC showing some features of minimal invasion without any features categorized in IC-IPMC was classified as MI-IPMC. I-IPMC showing at least one invasive feature beyond minimal invasion is classified as IC-IPMC. For example, if an I-IPMC shows mucous rupture and infiltrative growth of tubular adenocarcinoma with 6-mm length of invasion, this tumor is diagnosed as IC-IPMC.

An infiltrative growth pattern, which is commonly found in conventional invasive ductal carcinoma of the pancreas, is considerably aggressive (Figs. 1A–D). Among the 6 patients with IC-IPMC, in whom the depth of infiltration of carcinoma cells ranged from 6 to 20 mm, 3 patients (including a patient with 6-mm-length infiltration of carcinoma cells) had recurrence in the liver or peritoneal cavity, and died of the disease. This suggests that infiltrative growth is strongly associated with a high rate of recurrence and mortality, even if the size of invasion is limited. On the other hand, none of the 17 patients with a maximum infiltration of 5 mm or less had recurrence except 2 patients, 1 of them had 2-mm-length infiltration of tubular adenocarcinoma and the other had 2-mm-length infiltration of pure mucinous carcinoma. Therefore, we adopted a threshold of 5 mm as a diagnostic criterion for minimal invasion in infiltrative growth (Table 1). Lymphatic, venous, and neural invasion are treated as a part of infiltration of cancer cells. Invasion of 5 mm or less is sometimes difficult to detect. In such cases, elastica staining was helpful for differentiating infiltrating carcinoma from intraductal spreading of carcinoma (Figs. 1C, D).

IPMN is characterized by its prominent mucus secretion into the lumen, in some cases, into the space between epithelial cells and basement membrane due to inverted cellular polarity, which subsequently causes disruption of the pancreatic duct wall and spilling of mucus into the interstitial space.[1,7] This is referred to mucous rupture (Fig. 2) and is diagnosed as minimal invasion if mucous lakes are not associated with mucinous carcinoma showing infiltrative growth (Table 1). Mucous rupture was observed only in the vicinity of the pancreatic ductal system, although the location was not confined to the pancreas. We considered mucus lakes near noninvasive IPMC as mucous rupture regardless of the presence of viable cancer cells within it, because viable cancer cells may be present floating in the mucus lake. When viable cancer cells floating in mucus lake are apparently present and are scant (there is very small number of cancer cells or their clusters floating in only the limited mucus lakes. The representative feature was shown in Fig. 2D), this situation is called as "mucous rupture with cellular component." This subcategory includes a kind of pure mucinous carcinoma (alternatively colloid carcinoma)[1] showing a very low cellularity, and nonmucinous cancer cells which are simply detached from the duct wall and are floating in mucus lake. Mucous rupture without floating cancer cells represented the suspected lesion of mucous rupture with cellular component. When there are many cancer cells (more than "scant" level) floating in mucus lake, it is judged as infiltrative growth of mucinous carcinoma (Figs. 2E, F).

TABLE 1. Growth Patterns of I-IPMCs and Diagnostic Criteria for Minimal Invasion

Growth Pattern	Pathologic Features	Minimal Invasion	Beyond Minimal Invasion (IC-IPMC)
Infiltrative growth	Carcinoma cells from the pancreatic duct occupied by IPMC invade the surrounding stroma. Disappearance of the basement membrane or desmoplastic change around the ducts implies interstitial invasion. Infiltrative distance is defined as the length from the deepest point of invasion to the stroma surface of the nearest non-invasive IPMC	1. An infiltrative distance of 5 mm or less is regarded as minimal invasion 2. Venous, lymphatic, or neural invasion within the area ($\leq$5 mm of the infiltrative distance) is also counted in this category 3. This category includes the invasion of various histologic types of cancer, such as tubular adenocarcinoma, mucinous carcinoma, etc	1. An infiltrative distance more than 5 mm is regarded as IC-IPMC 2. Venous, lymphatic, or neural invasion within the area ($>$ 5 mm of the infiltrative distance) is also counted in this category 3. This category includes the invasion of various histologic types of cancer, such as tubular adenocarcinoma, mucinous carcinoma, etc
Mucous rupture	"Mucous rupture" and "expansive growth" are unique features of IPMC that grows intraductally and secretes large amounts of mucus. The mucus spills out, forming a mucus lake around the pancreatic duct, due to rupture of the dilatated pancreatic duct occupied by IPMN through high pressure caused by the hypersecreted mucin. This is referred to mucous rupture. Mucous lakes of various sizes are seen, sometimes containing scanty floating cancer cells	1. If mucous lakes are not associated with mucinous carcinoma showing infiltrative growth, this feature is diagnosed as minimal invasion, regardless of the size and location of the mucus lakes 2. If a mucus lake contains scanty floating cancer cells (there is very small number of cancer cells or their clusters floating in only the limited mucus lakes. The representative feature was shown in Fig. 2D), it is additionally described as "mucous rupture with cellular component." This subcategory includes a kind of pure mucinous carcinoma associated with IPMC 3. If many cancer cells (more than "scant" level) are floating in mucus lakes (Fig. 2E), it is treated as "infiltrative growth" of mucinous carcinoma and the infiltrative distance of 5 mm or less is regarded as minimal invasion	1. If many cancer cells are floating in mucus lakes, it is treated as "infiltrative growth" of mucinous carcinoma and the infiltrative distance of more than 5 mm is classified as IC-IPMC
Expansive growth	A pancreatic duct is markedly dilated, becoming ductectatic or cystic in shape. The basement membrane and subepithelial elastic fibers may be elongated and disrupted. Cystic IPMC may grow expansively into peripancreatic connective tissues, and eventually involves the bowel or major vessels [portal vein (PV), SPV, SMV, or splenic artery (SPA)]	1. Loss of the basement membrane of the pancreatic duct with IPMC is regarded as minimal invasion 2. If I-IPMC grows expansively, even if it ruptures into the bowel, or even if it erodes a major vessel wall unless cancer cells enter the lumen of the major vessel, it is still regarded as minimal invasion 3. If I-IPMC has this type of growth as predominance, it is corresponded to a kind of pure mucinous carcinoma associated with IPMC	1. If I-IPMC forms a fistula with a major vessel, it is regarded as IC-IPMC
Intra-abdominal rupture	IPMC ruptures into the abdominal cavity, and mucus-secreting cancer cells are scattered in it	Peritoneal dissemination may occur. Therefore, this finding should be distinguished from ordinary IPMN and classified separately as ruptured IPMN. MI- or IC-IPMC should be noted additionally	
Judgement		An I-IPMC showing some features of minimal invasion without any features categorized in IC-IPMC is classified as MI-IPMC	An I-IPMC showing at least one invasive feature beyond minimal invasion is classified as IC-IPMC

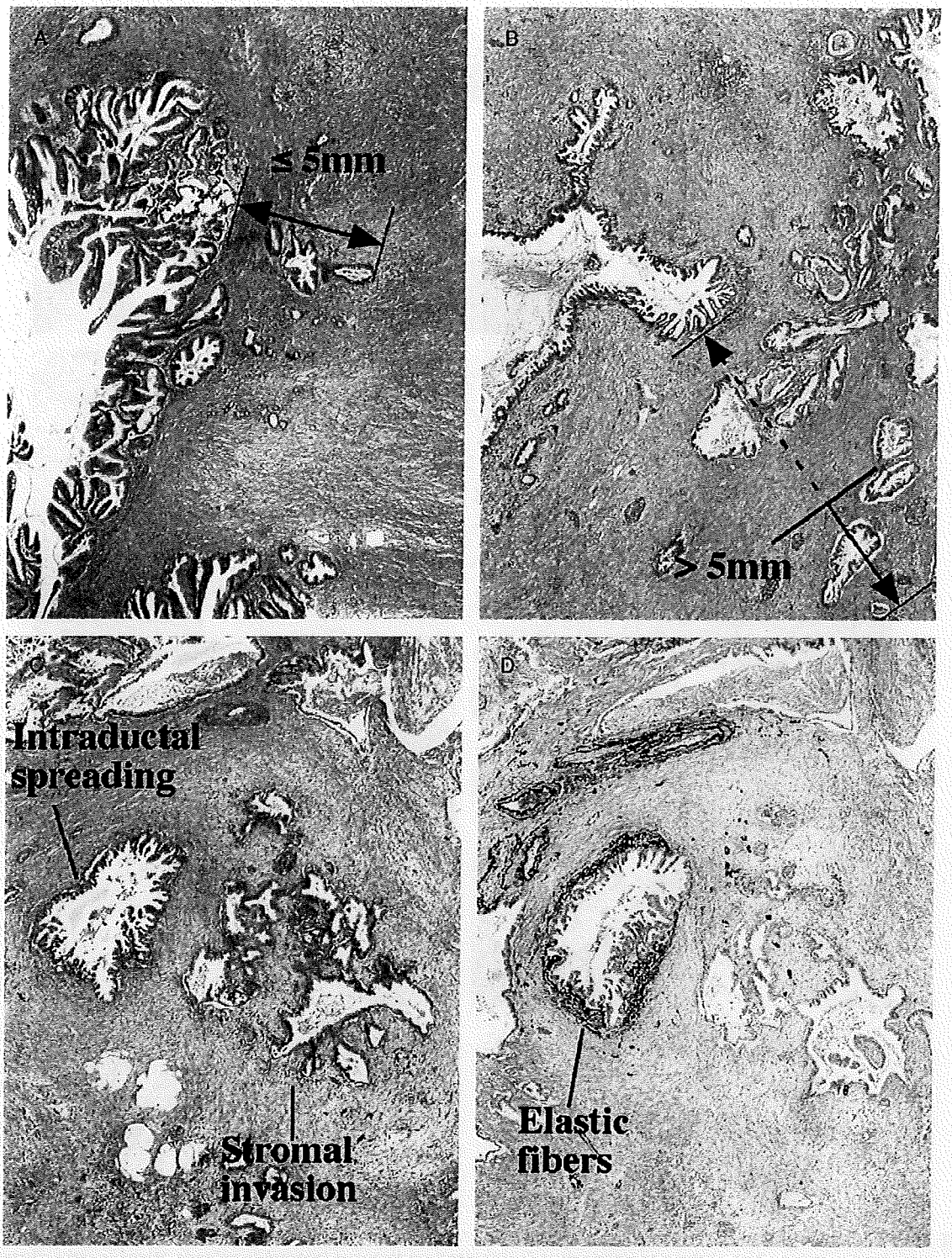

FIGURE 1. Histopathologic features of "infiltrative growth" in I-IPMC. A and B, Histologic features resemble those of conventional invasive ductal carcinoma of the pancreas. The arrows indicate the depth of infiltration of invasive carcinoma. If the depth is less than 5 mm, it is regarded as minimal invasion (A), and if the depth is more than 5 mm it is regarded as IC-IPMC (B). C and D, Elastica stain (D) helps to discriminate infiltrative growth from intraductal spread of carcinoma. The former lacks a positively stained sheath of elastic fibers (black) around the pancreatic duct. Hematoxylin and eosin stain (C).

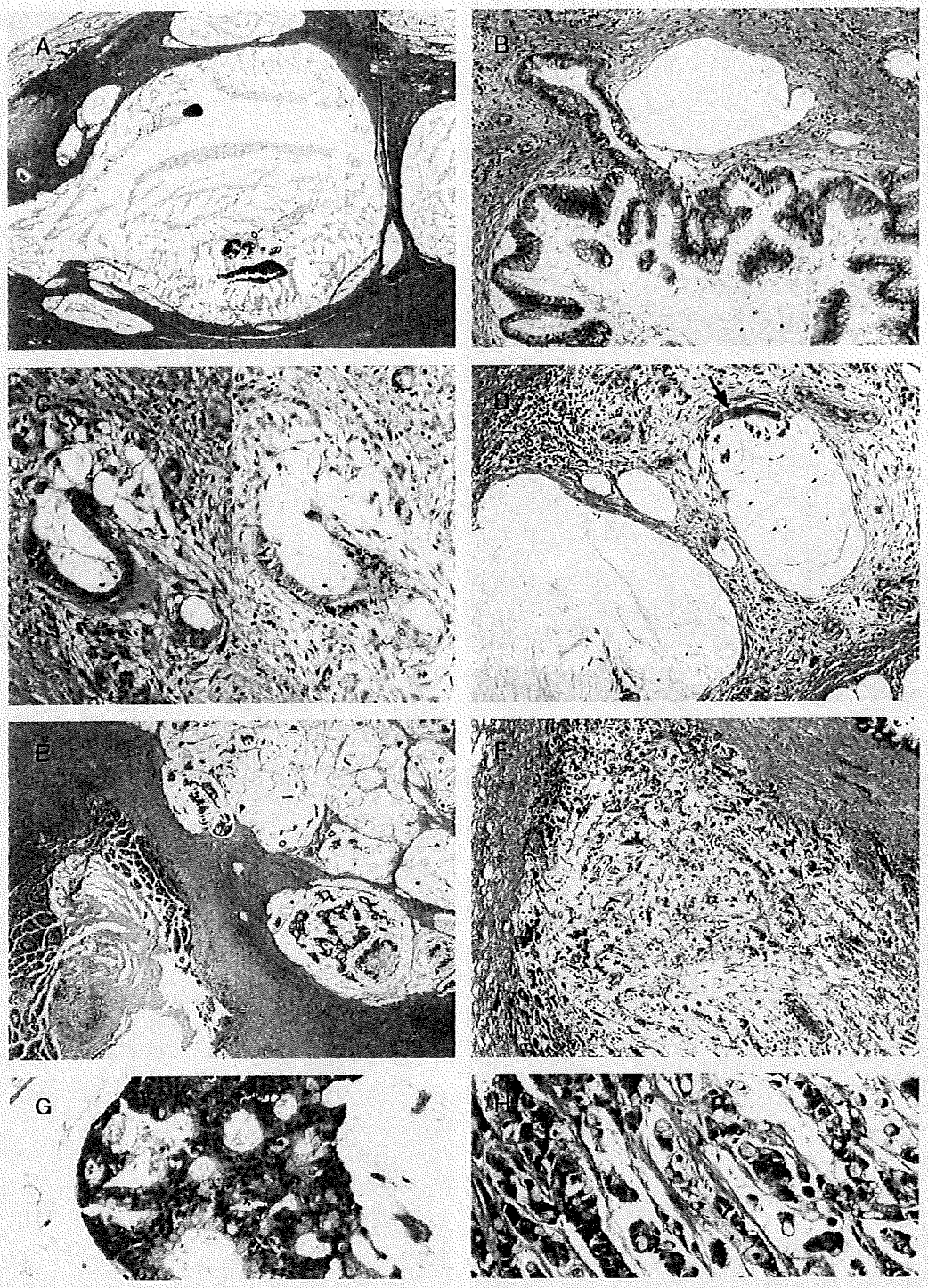

FIGURE 2. Histopathologic features of "mucous rupture" and "infiltrative growth" of mucinous carcinoma in I-IPMC. A to D, "Mucous rupture" pattern. Part of the pancreatic duct is disrupted and mucus leakage is evident. Variable sizes of mucus lakes without viable cancer cells floating are observed (A–C). A small duct covered by elastic fibers (C right column; elastica stain) is broken and the mucus leaks to form mucus lake (C). A small number of cancer cells (arrow) are floating in mucus lakes, which is described as "mucous rupture with cellular component." We could not observe any floating cancer cells in mucus lakes other than this cluster of cancer cells (arrow) in the entire lesion of the I-IPMC (D). E to H, "Infiltrative growth" of mucinous carcinoma. Many cancer cells floating in mucus lakes (E, G) or infiltrating features of mucinous carcinoma (F, H) are categorized as "infiltrative growth" of mucinous carcinoma. G and H, High-power view of (E) and (F), respectively.